

How charming can the Higgs be?

Artemis Sofia Giannakopoulou,^a Patrick Meade^a and Mauro Valli^b

^a*C.N. Yang Institute for Theoretical Physics, Stony Brook University, Stony Brook, NY 11794, USA*

^b*INFN Sezione di Roma, Piazzale Aldo Moro 2, I-00185 Rome, Italy*

E-mail: artemissofia.giannakopoulou@stonybrook.edu,
patrick.meade@stonybrook.edu, mauro.valli@roma1.infn.it

ABSTRACT: The coupling of the Higgs boson to first and second generation fermions has yet to be measured experimentally. There still could be very large deviations in these couplings, as the origin of flavor is completely unknown. Nevertheless, if Yukawa couplings are modified, especially for light generations, there are generically strong constraints from flavor-changing neutral currents (FCNCs). Therefore, it is imperative to understand whether there exists viable UV physics consistent with current data that motivates future Higgs coupling probes. In particular, the charm-quark Yukawa is the next quark coupling that could be measured at the LHC *if* it is a few times larger than the SM and compatible with flavor data. This is difficult to achieve in the context of standard ansatz such as Minimal Flavor Violation. In this paper we show that within the framework of Spontaneous Flavor Violation (SFV), using a Two Higgs Doublet Model as an example, the Higgs can be sufficiently charming that new LHC probes are relevant. In this charming region, we show that new Higgs states near the EW scale with large couplings to quarks are required, providing complementary observables or new constraints on the SM Yukawa couplings. The down-type SFV mechanism enabling the suppression of FCNCs also allows for independent modifications to the up-quark Yukawa coupling, which we explore in detail as well.

1 Overview

The study of Flavor Changing Neutral Currents (FCNCs) and CP violation in the Standard Model (SM) naively points to a scale of New Physics (NP) orders of magnitude greater than the electroweak (EW) one, beyond the reach of current and future colliders [1, 2]. From the perspective of Effective Field Theories (EFT), while the resolution of the SM flavor puzzle might be postponed to a very high ultraviolet (UV) scale, the SM renormalization group is still expected to induce, in general, effects of the Minimal Flavor Violation (MFV) type at low energy [3, 4]. The MFV ansatz allows maximal conservation of the $U(3)^5$ flavor group: as a consequence, the phenomenological impact of indirect searches is minimized [5–7], leaving room for a NP scale within the sensitivity of direct searches [8–12]. This result undoubtedly makes the MFV framework very popular among Beyond the SM (BSM) practitioners [13–15]. On the other hand, a MFV scenario corresponds to a highly non-generic situation: the UV theory must be indeed protected against any additional spurion over the Yukawa couplings which break the $U(3)^5$ flavor group in the SM. Notice that this statement must non-trivially translate into selection rules applying also to the CP-violating sector of the BSM scenario. In fact, as a result of SM precision tests such as the unitarity triangle, new $\mathcal{O}(1)$ phases over the one in the Cabibbo-Kobayashi-Maskawa (CKM) matrix can easily push the scale of NP above 100 TeV [16].

An unavoidable outcome of inheriting the hierarchies of the SM Yukawa couplings is that all MFV models feature NP couplings to the third generation as the main phenomenological driver for BSM searches at the Large Hadron Collider (LHC). While this fact might align well with arguments in favor of the EW hierarchy problem [17, 18], the MFV ansatz automatically induces a strong bias into the set of interesting experimental targets at stake for the present and future High Energy frontier. In the absence of hints for top partners or other BSM physics, it is crucial today more than ever to explore alternatives to the MFV paradigm. This is especially true in the Higgs precision measurements of Yukawa couplings and the search for evidence of yet unmeasured ones.

Observation of Yukawa couplings gives the first direct probe into the origin of known flavor within the SM. However, this direct probe is experimentally very challenging at the LHC. Reliable flavor identification outside of the leptonic sector is mostly restricted to heavy quarks. Furthermore, the small size of first and second generation lepton Yukawa couplings means that despite the experimental ability for particle identification, current LHC datasets are not sufficient for measurements. In particular, only the coupling of the Higgs to the third generation of matter has been experimentally observed thus far [19]. Future running of the LHC and its extension, the HL-LHC, should enable the observation of the SM coupling of the Higgs to the muon. However, even with the HL-LHC, measuring the first- or second-generation couplings of the quarks to the Higgs remains extremely challenging.

The next closest “observation” of flavor in the quark sector – and therefore the most tantalizing target at present – is certainly the charm-quark Yukawa. This has motivated many recent studies from ATLAS and CMS [20–33], as well as current HL-LHC projections, showing that it may be possible to probe within a factor of a few times the SM

charm Yukawa coupling [19]. This has also led to a large amount of theoretical activity exploring a variety of observables that potentially enhance the sensitivity of the LHC, some of which have been incorporated into the aforementioned results. These include better attempts at flavor tagging and understanding the exclusive radiative decays into charmed mesons [34], looking for associated charm production [35], incorporating the sensitivity of the p_T spectrum of the Higgs [36] or the correlated $h + \gamma$ production [37], and combinations of techniques and channels [38–42] (see also references therein). As of now, even with the concerted theoretical effort and the most advanced experimental analyses based on machine-learning algorithms, the best chance for an observation in this channel seems to require an $\mathcal{O}(1)$ enhancement of the charm Yukawa, putting it well beyond the natural regime of MFV. If we consider typical models of flavor beyond the SM, it is often difficult to enhance the charm Yukawa significantly without running into other constraints, see e.g., the case study in Ref. [15]. Therefore, it is imperative to explore alternatives to understand if there are motivated possibilities that can be explored by the LHC. One such framework that was previously investigated for down-type quark Yukawa couplings is Spontaneous Flavor Violation (SFV) [43].

SFV can be viewed as symmetry protected subset of Aligned Flavor Violation (AFV). AFV is achieved by introducing spurions of the maximal SM flavor group as an expansion in powers of the CKM matrix, with expansion coefficients diagonal in flavor space to ensure invariance under rephasing of SM fermion fields [44, 45]. Generically, the individual quark-flavor number symmetries are not sufficient to leave phenomenological room for low-scale flavored new degrees of freedom [43, 46–48]. SFV allows for low-scale flavored BSM physics by postulating a CP and family symmetry that is only broken via wavefunction renormalization of right-handed up quarks *or* down quarks [43]. This symmetry breaking pattern allows for enough protection to be phenomenologically viable from indirect constraints while opening up new opportunities at colliders. In practice one can roughly view SFV as having a new diagonal BSM spurion for *either* up-type *or* down-type quark couplings, as there are up-type or down-type SFV models¹. Interestingly, such theories can also enjoy further phenomenological motivation in correspondence to the resolution of the strong CP problem [49–52].

If one applies SFV to a Two Higgs Doublet Model (2HDM), this extends 2HDMs beyond the typical four discrete choices implied by Natural Flavor Conservation and allows for EW scale states that couple with fundamentally different patterns to quark flavors. In [53, 54] the up-type version of a SFV 2HDM was studied and, in particular, if mixing is allowed, it lead to significant enhancements in the down and strange Yukawa couplings of the SM Higgs. In the context of a flavor model, this also allows for the correlation of the SM Higgs Yukawa with additional observables. For instance, a mixing between Higgses in combination with new Yukawas of a heavy second Higgs implies a new type of di-Higgs signature [54], which for the down and strange Yukawa couplings sets strongest bounds.

In this paper we extend the analysis to the SFV down-type 2HDM where significant

¹This refers to sector where symmetry breaking occurs, while the new BSM spurion resides in the opposite quark sector.

enhancements of the charm Yukawa are possible. This is crucial for two main reasons. First, it is important to determine if there are perturbatively describable models compatible with indirect flavor bounds that the LHC could detect through a charm Yukawa measurement. Second, in models that permit a significant enough deviation in the charm Yukawa coupling to be measurable, we need to assess whether this measurement is the optimal observable. Alternatively, we must consider if the relevant parameter space for charm Yukawa sensitivity is already excluded by other LHC observables.

Our main finding here is that in the context of SFV 2HDM models there is a viable parameter space where a charm Yukawa could be observable at the LHC while satisfying all current bounds. Furthermore, as with up-type SFV models [54] multiple observables beyond charm specific ones may be as sensitive as single-Higgs properties. Therefore, a key lesson from our study is that a concerted effort across searches and precision measurements is recommended to extract the maximal LHC reach for BSM physics.

The paper is organized as follows. In [section 2](#) we introduce the class of 2HDMs realizing SFV. In [section 3](#) and [section 4](#) we discuss and derive the main results of our work, namely the constraints on the parameter space of the down-type SFV 2HDM, coming from flavor and collider physics respectively. Additional indirect constraints such as EW precision tests are subleading since 2HDM models naturally preserve a custodial symmetry [55], and as discussed in [section 2](#) we work in the CP-conserving version of the model for simplicity. We then compare with the results from Higgs precision measurements in [section 5](#) to understand how complementary these measurement are, and whether there is relevant parameter space that can be explored with flavor tagging measurements at the LHC. Finally, in [Appendix A](#) we update the bounds on up-type SFV 2HDM and we leave our conclusions to [section 6](#). For the sake of completeness, in [Appendices B](#) and [C](#) we report the loop functions relevant to this study and collect the couplings of the Higgs particles to SM fermions.

2 Spontaneous Flavor Violating 2HDM

Following the SFV prescription described in [section 1](#), in this study we work with a specific class of models realizing it, namely 2HDMs endowed with the SFV ansatz. We illustrate how well-motivated BSM benchmarks that are not flavorless or mostly interacting via the third-generation fermions can be probed by experiments.

The Higgs sector of a 2HDM is extended compared to the Standard Model by adding a second Higgs doublet with the same hypercharge as the SM one. It is convenient to work in the Higgs basis [56], where only one of the two doublets has a non-zero vacuum expectation value. Choosing $\langle H_1 \rangle \neq 0$ and $\langle H_2 \rangle = 0$, we can write:

$$H_1 = \begin{pmatrix} G^+ \\ \frac{1}{\sqrt{2}} (v + H_1^0 + iG^0) \end{pmatrix}, \quad H_2 = \begin{pmatrix} H^+ \\ \frac{1}{\sqrt{2}} (H_2^0 + iA) \end{pmatrix}. \quad (2.1)$$

Here we denote the Goldstone bosons by G^0 and G^\pm . In this extended scalar sector we have five mass eigenstates. We will denote by H^\pm the charged Higgs eigenstate, A the

CP-odd one, H_1^0 and H_2^0 the fields mixing into the CP-even light and heavy neutral Higgs:

$$\begin{aligned} h &= H_1^0 \sin(\beta - \alpha) + H_2^0 \cos(\beta - \alpha), \\ H &= H_1^0 \cos(\beta - \alpha) - H_2^0 \sin(\beta - \alpha), \end{aligned} \quad (2.2)$$

where $\cos(\beta - \alpha)$ is the alignment parameter. According to what was reported above, in what follows we shall identify h with the 125 GeV Higgs resonance observed at the LHC.

The Higgs sector of the Lagrangian of the models considered in this work is given by:

$$|D_\mu H_a|^2 - V(H_1, H_2) - \left(\mathcal{Y}_{aij}^u \bar{Q}_{Li} H_a U_{Rj} + \mathcal{Y}_{aij}^d \bar{Q}_{Li} H_a^c D_{Rj} + \mathcal{Y}_{aij}^\ell \bar{L}_{Li} H_a^c \ell_{Rj} + h.c. \right), \quad (2.3)$$

where we denote with \mathcal{Y}_{aij}^f the Yukawa matrices of our model, with $f = u, d, \ell$ denoting up-type, down-type quarks and leptons respectively. The index $a = 1, 2$ runs over the two distinct Higgs doublets. The potential $V(H_1, H_2)$ in the Higgs basis reads as:

$$\begin{aligned} V(H_1, H_2) &= m_1^2 H_1^\dagger H_1 + m_2^2 H_2^\dagger H_2 + \left(m_{12}^2 H_1^\dagger H_2 + h.c. \right) + \frac{1}{2} \lambda_1 \left(H_1^\dagger H_1 \right)^2 \\ &+ \frac{1}{2} \lambda_2 \left(H_2^\dagger H_2 \right)^2 + \lambda_3 \left(H_1^\dagger H_1 \right) \left(H_2^\dagger H_2 \right) + \lambda_4 \left(H_1^\dagger H_2 \right) \left(H_2^\dagger H_1 \right) \\ &+ \left\{ \frac{1}{2} \lambda_5 \left(H_1^\dagger H_2 \right)^2 + \left[\lambda_6 \left(H_1^\dagger H_1 \right) + \lambda_7 \left(H_2^\dagger H_2 \right) \right] \left(H_1^\dagger H_2 \right) + h.c. \right\}. \end{aligned} \quad (2.4)$$

The alignment angle related to the physical Higgs states can be expressed via the parameters appearing in Eq. (2.4), namely:

$$\tan[2(\beta - \alpha)] = \frac{2\lambda_6 v^2}{\lambda_1 v^2 - \left(m_2^2 + \frac{1}{2}(\lambda_3 + \lambda_4 + \lambda_5) v^2 \right)}. \quad (2.5)$$

In the limit $\cos(\beta - \alpha) \rightarrow 0$, the SM Higgs field h resides entirely in one of the two Higgs doublets. This regime is called the *aligned limit* of the theory. We can tune the parameters of our theory such that the model is in this regime by setting in Eq. (2.5) $m_2 \rightarrow \infty$ (*decoupling limit*) or $\lambda_6 \rightarrow 0$ (*alignment without decoupling*).

In our study we work with $\cos(\beta - \alpha) \neq 0$, i.e. assuming both terms are present in each line of Eq. (2.2). Indeed, when the alignment parameter is non-zero, deviations from the SM predictions for the Higgs couplings are expected and can be interestingly probed by current measurements [57]. In this work, we are interested in exploring the small but non-zero $\cos(\beta - \alpha)$, such that we remain relatively close to the SM. Additionally, for simplicity, we assume that the new Higgs eigenstates are degenerate, i.e., $\lambda_4, \lambda_5 \rightarrow 0$, such that $m_H = m_{H^\pm} = m_A$. We will maintain this assumption of degenerate masses throughout the rest of this analysis. Under these conditions, we can write the following expansion for the alignment parameter [58, 59]:

$$\cos(\beta - \alpha) = -|\lambda_6| \frac{v^2}{m_H^2} + \mathcal{O}\left(\frac{v^4}{m_H^4}\right), \quad (2.6)$$

where λ_6 is given in equation (2.4). Assuming a small but non-zero mixing between the two Higgs doublets, we can use Eq. (2.6) to estimate the range of masses, m_H , for which

the coupling λ_6 remains finite. To avoid Landau poles at the TeV scale, we set an upper limit of $m_H \leq 2\text{TeV}$. Within this mass range and for a small alignment parameter, λ_6 stays within the perturbative regime [53].

For the sake of minimality, in the present analysis we do not introduce any additional phases apart from the CKM one, working with a CP-conserving SFV 2HDM. Also, notice that without loss of generality we can always rotate the Higgs potential in Eq. (2.4) to the Peccei-Quinn basis where the couplings and masses are real.

As anticipated in section 1, an important characterization for the phenomenology of the SFV 2HDM is whether the alignment in flavor space goes along with the SM down-type or up-type Yukawa matrix. For instance, in the case of alignment with the down-quark sector, the up-quark fields will need to be rotated to the mass eigenstates according to:

$$Q = \begin{pmatrix} V^\dagger u \\ d \end{pmatrix}, \quad (2.7)$$

where we denote by V the CKM matrix. Following the spurion language of [43], for the *down-type* SFV, there will be no new flavor violating spurions transforming under $U(3)_Q \times U(3)_d$ appearing in renormalizable interactions. However, new flavor aligned spurions non-trivial under $U(3)_Q \times U(3)_u$ will be allowed. In such a case, the couplings to the Higgs doublet H_1 will read as:

$$\mathcal{Y}_1^u = V^* \text{diag}(y_u, y_c, y_t) \equiv V^* Y^u, \quad \mathcal{Y}_1^d = -Y^d, \quad \mathcal{Y}_1^\ell = -Y^\ell, \quad (2.8)$$

while Yukawa matrices dictating the couplings of the second Higgs doublet H_2 will be:

$$\mathcal{Y}_2^u = V^* \text{diag}(\lambda_u, \lambda_c, \lambda_t) \equiv V^* \Lambda^u, \quad \mathcal{Y}_2^d = -\xi Y^d, \quad \mathcal{Y}_2^\ell = -\xi^\ell Y^\ell, \quad (2.9)$$

where we denote by Y^f the (diagonal) SM Yukawa matrices with $f = u, d, \ell$ depending on the coupling to up- or down-type quarks or to leptons. Using Eq.s (2.8) – (2.9), we can derive the couplings of the Higgs eigenstates to the quarks and leptons, getting for example for the lightest CP even Higgs,

$$\mathcal{Y}_{u_i \bar{u}_j}^h = \delta_{ij} [y_{u_j} \sin(\beta - \alpha) + \lambda_{u_j} \cos(\beta - \alpha)]. \quad (2.10)$$

The rest of the Higgs mass eigenstates couplings are listed in Appendix C. Note that $\lambda_u, \lambda_c, \lambda_t$ are new, independent Yukawa couplings of H_2 to the up-type quarks.² We emphasize that these BSM couplings are not bound to follow the SM hierarchy and the second Higgs doublet H_2 is allowed to couple to the quarks with different coupling size than the SM analogue. In Eq. (2.9), ξ and ξ^ℓ are constants that control the size of the couplings of the second Higgs doublet to the down-type quarks and leptons, respectively.³ As mentioned before, they are required to be real since we don't allow for new sources of CP violation. Finally, couplings to gauge bosons follow the standard literature on 2HDM [59].

In a similar fashion, one can define the case of an *up-type* SFV 2HDM where new Higgs couplings to the down-quark sector are not forbidden a priori and will impact the

²Not to be confused with the couplings appearing in Eq. (2.4), denoted by λ_i with $i = 1, \dots, 6$.

³In our analysis we study in detail the quark sector and we set for simplicity $\xi^\ell = 0$.

phenomenology [53]. While we will update also the available bounds for that scenario in Appendix A, the primary focus of this study will be on the constraining power of the charm coupling modifier κ_c , according to the definition:

$$\kappa_{q_i} \equiv \mathcal{Y}_{q_i \bar{q}_i}^h / y_{q_i} , \quad (2.11)$$

where we denote with y_{q_i} the coupling of the Higgs within the SM to the quark q with flavor i , and with $\mathcal{Y}_{q_i \bar{q}_i}^h$ the corresponding one in the mass basis of the 2HDM, as explicitly reported in Eq. (2.10). Therefore, we will primarily explore the *down-type* SFV 2HDM scenario. In the following, we will first present the most relevant bounds from and then move to inspect the constraints coming from direct searches at colliders.

3 Bounds from FCNC processes

Rare B decays and neutral meson oscillations are precisely measured FCNC processes, which can provide crucial tests of the SM. As in the SM, in SFV theories FCNCs do not appear at tree level. Nevertheless, also for the class of models analyzed here $\Delta F = 1, 2$ FCNC transitions offer the most relevant constraints for what concerns indirect searches [53]. Using an EFT approach, the relevant Wilson coefficients for the generated dimension-six operators can be computed for the SFV 2HDM under scrutiny. Adopting up-to-date measurements and theory predictions of the most recent literature – reported in table 1 – we can restrict the available parameter space of the new Yukawa couplings λ_u , λ_c , λ_t .

3.1 Bounds from rare B decays

The inclusive radiative B -meson decays are well-known to provide leading constraints on the parameter space of 2HDMs [65]. In our class of 2HDMs, $B \rightarrow X_{s,d} \gamma$ arise at one loop as shown in figure 1: NP contributions to these processes can be mediated by either charged or neutral Higgs eigenstates. In the case of down-type SFV, working with an operator product expansion at mass dimension six, the effective weak Hamiltonian involves the same set of operators of the SM one [66]; for $b \rightarrow s \gamma$, e.g., we can write:

$$\mathcal{H}_{eff}^{b \rightarrow s \gamma} = -\frac{4G_F}{\sqrt{2}} V_{tb} V_{ts}^* \sum_i C_i \mathcal{O}_i , \quad (3.1)$$

where the sum is indeed over current-current, QCD and QED penguin and dipole operators. In particular, the leading phenomenological contributions to the process from the down-type SFV 2HDM are given by the matching onto the electromagnetic and chromomagnetic dipole operators that are not chirally suppressed by the light-quark mass, namely:

$$\begin{aligned} \mathcal{O}_7 &= \frac{e}{16\pi^2} m_b \bar{s} \sigma^{\mu\nu} P_R b F_{\mu\nu} , \\ \mathcal{O}_8 &= \frac{g_s}{16\pi^2} m_b \bar{s} \sigma^{\mu\nu} T^a P_R b G_{\mu\nu}^a . \end{aligned} \quad (3.2)$$

The Wilson coefficients corresponding to the operators in Eq. (3.2) can be explicitly

Observable	Constraint	95% probability range	Ref.
$b \rightarrow s\gamma$	C_7 C'_7	$[-0.062, 0.040]$ $[-0.30, 0.30]$	[60, 61]
$b \rightarrow d\gamma$	C_7 C'_7	$[-0.11, 0.20]$ $[-0.41, 0.41]$	[62, 63]
$b \rightarrow s\mu^+\mu^-$	C_{10}	$[-0.15, 0.62]$	[64]
$K - \bar{K}$	$Re(C_1)$ $Im(C_1)$	$[-6.8, 7.7] \times 10^{-13} \text{ GeV}^{-2}$ $[-1.2, 2.4] \times 10^{-15} \text{ GeV}^{-2}$	[5, 16]
$B_s - \bar{B}_s$	$ C_1 $	$< 1.9 \times 10^{-11} \text{ GeV}^{-2}$	[5, 16]
$B_d - \bar{B}_d$	$ C_1 $	$< 9.5 \times 10^{-13} \text{ GeV}^{-2}$	[5, 16]
$D - \bar{D}$	$Re(C_1)$ $Im(C_1)$	$[-2.5, 3.1] \times 10^{-13} \text{ GeV}^{-2}$ $[-9.4, 8.9] \times 10^{-15} \text{ GeV}^{-2}$	[5, 16]

Table 1: Most important constraints in our analysis from indirect searches. We list the available limits on the Wilson coefficients at a matching scale close to the EW one. Notice that C'_7 and $D - \bar{D}$ bounds are relevant only for up-type SFV studied in the Appendix A.

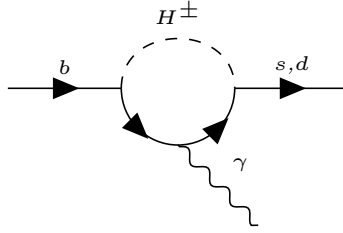


Figure 1: Example of penguin diagram for SFV 2HDM contributing to inclusive radiative B decays. Notice that non-negligible effects from the fermion in the loop can arise a priori from any up-type quark on the basis of the size of the new Yukawa couplings of the theory.

calculated for our model [66] using the couplings in Appendix C. They are presented below as functions of the relevant SM and BSM parameters:

$$C_7 = \frac{v^2}{V_{tb}V_{ts}^*} \sum_{j=u,c,t} \left(\frac{1}{m_b} \mathcal{Y}_{sj}^{H^{+*}} \mathcal{Y}_{jb}^{H^-} \frac{C_{7,XY}^0(z_j)}{m_j} + \mathcal{Y}_{sj}^{H^{+*}} \mathcal{Y}_{bj}^{H^+} \frac{C_{7,YY}^0(z_j)}{m_j^2} \right), \quad (3.3)$$

where $z_j \equiv m_j^2/m_H^2$ and the loop functions are reported for convenience in Appendix B. We can obtain the expressions for the Wilson coefficients of \mathcal{O}_8 by replacing the loop functions in Eq. (3.3) by $C_{8,XY}^0$ and $C_{8,YY}^0$, also reported in the same appendix. Eventually, the same loop functions also characterize the matching expression for the dipole operators

with opposite chirality with respect to the ones in Eq. (3.3) – which matter for the up-type SFV 2HDM – implying also a trivial change in the Yukawa couplings involved [67].

Using the latest experimental average for the branching ratio of the inclusive decay $B \rightarrow X_s \gamma$ – namely $\mathcal{B}_{s\gamma} = (3.49 \pm 0.19) \times 10^{-4}$ [61] – and adopting the theoretical prediction updated in Ref. [60], we derive a bound on the 2HDM parameter space (m_H, λ_i) . Similarly, following what was recently worked out in Ref. [62] for $b \rightarrow d\gamma$, we investigate the bound from $B \rightarrow X_d \gamma$ in the same parameter space, adopting $\mathcal{B}_{d\gamma} = (14.1 \pm 5.7) \times 10^{-6}$ as the experimental constraint [63]. With no much of a surprise, the bound reported in table 1 highlights how the leading constraint comes from $b \rightarrow s\gamma$, whose theory prediction with respect to $b \rightarrow d\gamma$ is less sensitive to long-distance effects [67]. In particular, we find the driver of the bound to be the electromagnetic dipole, whose contribution to the branching ratio is a factor of four more relevant than the chromomagnetic contribution under QED \otimes QCD renormalization group, see the general phenomenological expressions given in [68] and the updated one for $b \rightarrow s\gamma$ in [60], where NP effects on the branching ratio are specifically reported for $\mathcal{O}_{7,8}$.

In addition to the radiative inclusive channel, a rare B -meson decay which provides today a precise indirect test of the short-distance physics of the SM is certainly $B_s \rightarrow \mu^+ \mu^-$ [69], particularly well-studied in the context of 2HDMs [70, 71]. Such a decay pertains to the partonic process $b \rightarrow s \mu^+ \mu^-$: within our flavor construction, tree-level diagrams that violate flavor are not allowed and the leading-order contributions to this class of FCNC transitions come at the one loop from Z penguins and new box diagrams involving charged Higgses, see figure 2. At dimension six, the effective Hamiltonian is the one given in Eq. (3.1) with the addition of the semileptonic operators:

$$\begin{aligned} \mathcal{O}_9 &= \frac{e^2}{16\pi^2} \bar{s} \gamma_\rho P_L b \bar{\mu} \gamma^\rho \mu , \\ \mathcal{O}_{10} &= \frac{e^2}{16\pi^2} \bar{s} \gamma_\rho P_L b \bar{\mu} \gamma^\rho \gamma_5 \mu , \end{aligned} \tag{3.4}$$

and their chirality-flipped version, which turn out to play a minor role in our study. Due to the quantum numbers characterizing \mathcal{O}_9 , sizable hadronic physics can plague a precise assessment of the short-distance contribution associated to this operator in a global analysis of $b \rightarrow s \ell^+ \ell^-$ transitions [72, 73]. As a consequence of this observation, a conservative bound on NP in C_9 points inevitably to a relatively weak constraint [64].

On the contrary, the absence of γ penguins in the effective coupling associated to \mathcal{O}_{10} underlies a robust probe of new short-distant effects, experimentally well constrained by the competitive measurement of the branching ratio for $B_s \rightarrow \mu^+ \mu^-$ performed independently by ATLAS, CMS and LHCb collaborations [61]. Using the couplings in Appendix C and the results collected in Ref. [74], we can write down the explicit expression for the Wilson coefficient of \mathcal{O}_{10} in our SFV 2HDM:

$$C_{10} = \frac{\mathcal{Y}_{sq}^{H^{*+}} \mathcal{Y}_{bq}^{H^+}}{2e^2 V_{qb} V_{qs}^*} (I_1(z_q) - 1) , \tag{3.5}$$

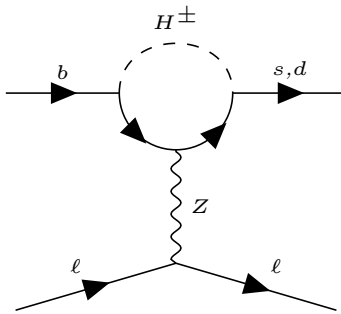


Figure 2: Example of penguin diagram for SFV 2HDM contributing to the short-distance physics of $b \rightarrow s, \mu^+ \mu^-$. Notice that the loop function of these contributions features an important suppression in the limit of very light quarks in the loop [75].

where $I_1(z_i)$ is a loop function given in Appendix B and $z_q = m_q^2/m_H^2$ with $q = u, c, t$. Notably, such a function vanishes in the limit of massless quarks, implying the relevance of the top quark running in the loop for the $B_s \rightarrow \mu^+ \mu^-$ in our model-building scenarios.

Using the bounds from rare B decays, we can map the allowed parameter space for the new Yukawa couplings of the second Higgs doublet. The results are presented in figure 4. The bounds are shown in terms of the mass of the heavy Higgs and the relevant new Yukawa coupling. For each panel, we chose to allow only one of the up-type Yukawas of the second Higgs doublet to be non-zero. This particular slicing of the parameter space is chosen in order to make the presentation of the results clear and highlight the role of these bounds for each of the three up-quark flavors.

The shape of the constraints depends on the couplings of the second Higgs doublet to the fermions. Modifying the proportionality constant ξ that relates the new down-type Yukawa matrix to the SM one, leads to different results for the bounds presented in figure 4. In that figure, we have chosen to set $\xi = 0$ for the sake of simplicity, bearing in mind that $\mathcal{Y}^{H^-} = -(\xi V^* Y^d) \neq 0$ would result in more Wilson coefficients becoming relevant. Furthermore, notice that the CKM insertions and quark masses multiplying the loop functions in the matching expression for the dipole operators are different when we choose to have a non-zero charm or top new Yukawa coupling. In this regard, for the case of the up-quark Yukawa, the loop functions in combination with the CKM elements that will appear in the expressions lead to a large suppression of the overall Wilson coefficient which consequently does not lead to interesting constraints on the parameter space.

For the case of the semi-leptonic operators entering in the effective Hamiltonian for $b \rightarrow s \mu^+ \mu^-$, Eq. (3.5), there is no term $\propto (\mathcal{Y}^{H^+} \mathcal{Y}^{H^-})$. As a result, there is no dependence on ξ for the bound from $B_s \rightarrow \mu^+ \mu^-$. Finally, notice also that since it is the charged Higgs eigenstate H^\pm which mediates these FCNC processes, meaning that the result will be independent of the alignment parameter $\cos(\beta - \alpha)$, as evident from what reported in Appendix C.

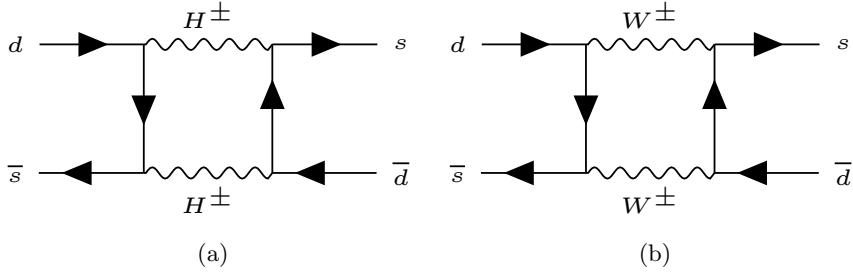


Figure 3: Example diagrams for $K - \bar{K}$ mixing. On the left we show the contribution mediated by the new charged Higgs eigenstates, next to the W -boson box diagram of the SM on the right. For the other $\Delta F = 2$ processes examined one obtains the relevant diagrams by properly changing the quark flavors of the initial and final states.

3.2 Bounds from neutral meson mixing

Meson-antimeson mixing offers the most stringent bounds on baryon- and lepton-number conserving NP [5, 6]. Continuing our analysis, we will now consider the constraints on the new Yukawas from the bounds on the Wilson coefficients of the $\Delta F = 2$ effective operators responsible of those FCNC processes.

The relevant Feynman diagrams are at the one-loop level, mediated by charged Higgs eigenstates or charged EW bosons, see the examples in figure 3. Then, the $\Delta F = 2$ effective weak Hamiltonian describing neutral meson mixing reads in full generality [1]:

$$\mathcal{H}_{eff}^{\Delta F=2} = \sum_{i=1}^5 C_i \mathcal{O}_i + \sum_{j=1}^3 C'_j \mathcal{O}'_j + h.c. , \quad (3.6)$$

where, e.g., in the case of $K - \bar{K}$ mixing, the effective operators are:

$$\begin{aligned} \mathcal{O}_1 &= (\bar{s}_\alpha \gamma_\mu P_L d_\alpha) (\bar{s}_\beta \gamma^\mu P_L d_\beta) , \\ \mathcal{O}_2 &= (\bar{s}_\alpha P_L d_\alpha) (\bar{s}_\beta P_L d_\beta) , \\ \mathcal{O}_3 &= (\bar{s}_\alpha P_L d_\beta) (\bar{s}_\beta P_L d_\alpha) , \\ \mathcal{O}_4 &= (\bar{s}_\alpha P_L d_\alpha) (\bar{s}_\beta P_R d_\beta) , \\ \mathcal{O}_5 &= (\bar{s}_\alpha P_L d_\beta) (\bar{s}_\beta P_R d_\alpha) , \\ \mathcal{O}'_1 &= (\bar{s}_\alpha \gamma_\mu P_R d_\alpha) (\bar{s}_\beta \gamma^\mu P_R d_\beta) , \\ \mathcal{O}'_2 &= (\bar{s}_\alpha P_R d_\alpha) (\bar{s}_\beta P_R d_\beta) , \\ \mathcal{O}'_3 &= (\bar{s}_\alpha P_R d_\beta) (\bar{s}_\beta P_R d_\alpha) , \end{aligned} \quad (3.7)$$

with $P_{L,R} = \frac{1}{2}(1 \mp \gamma_5)$ and α, β are color indices. Notice that for $D - \bar{D}$ and $B_{d,s} - \bar{B}_{d,s}$ meson mixing, the four-fermion operators of the corresponding $\Delta F = 2$ weak effective Hamiltonian need the appropriate change in the field flavor content in Eq. (3.7).

The corresponding one-loop Wilson coefficients are presented below in terms of the relevant masses, mixing angles and Yukawa couplings. The loop functions D_0 and D_2

involved in the $\Delta F = 2$ matching are reported in Appendix B. The Wilson coefficients for box diagrams with charged Higgs in the loops are [66]:

$$\begin{aligned}
C_1 &= \frac{-1}{128\pi^2} \sum_{j,k=1}^3 \mathcal{Y}_{d_1\bar{u}_j}^{H^{+*}} \mathcal{Y}_{d_2\bar{u}_j}^{H^+} \mathcal{Y}_{d_1\bar{u}_k}^{H^{+*}} \mathcal{Y}_{d_2\bar{u}_k}^{H^+} D_2(m_{u_j}^2, m_{u_k}^2, m_H^2, m_H^2), \\
C_2 &= \frac{-1}{32\pi^2} \sum_{j,k=1}^3 m_{u_j} m_{u_k} \mathcal{Y}_{u_j\bar{d}_1}^{H^{-*}} \mathcal{Y}_{d_2\bar{u}_j}^{H^+} \mathcal{Y}_{u_k\bar{d}_1}^{H^{-*}} \mathcal{Y}_{d_2\bar{u}_k}^{H^+} D_0(m_{u_j}^2, m_{u_k}^2, m_H^2, m_H^2), \\
C_4 &= \frac{-1}{16\pi^2} \sum_{j,k=1}^3 m_{u_j} m_{u_k} \mathcal{Y}_{u_j\bar{d}_1}^{H^{-*}} \mathcal{Y}_{d_2\bar{u}_j}^{H^+} \mathcal{Y}_{d_1\bar{u}_k}^{H^{+*}} \mathcal{Y}_{u_k\bar{d}_2}^{H^-} D_0(m_{u_j}^2, m_{u_k}^2, m_H^2, m_H^2), \\
C_5 &= \frac{1}{32\pi^2} \sum_{j,k=1}^3 \mathcal{Y}_{u_j\bar{d}_1}^{H^{-*}} \mathcal{Y}_{u_j\bar{d}_2}^{H^-} \mathcal{Y}_{d_1\bar{u}_k}^{H^{+*}} \mathcal{Y}_{d_2\bar{u}_k}^{H^+} D_2(m_{u_j}^2, m_{u_k}^2, m_H^2, m_H^2),
\end{aligned} \tag{3.8}$$

and by replacing $\mathcal{Y}^{H^+} \leftrightarrow \mathcal{Y}^{H^-}$ we obtain the coefficients of the primed operators. For the processes via charged Higgs and W or Goldstone exchange, one gets [66]:

$$\begin{aligned}
C_1 &= \frac{-1}{128\pi^2} \frac{g^2}{m_W^2} \sum_{j,k=1}^3 V_{j1}^* V_{k2} m_{u_j} m_{u_k} \mathcal{Y}_{d_2\bar{u}_j}^{H^+} \mathcal{Y}_{d_1\bar{u}_k}^{H^{+*}} \left[D_2(m_{u_j}^2, m_{u_k}^2, m_W^2, m_H^2) \right. \\
&\quad \left. - 4m_W^2 D_0(m_{u_j}^2, m_{u_k}^2, m_W^2, m_H^2) \right], \\
C_1' &= \frac{-1}{128\pi^2} \frac{g^2}{m_W^2} \sum_{j,k=1}^3 V_{j1}^* V_{k2} m_s m_d \mathcal{Y}_{u_j\bar{d}_2}^{H^-} \mathcal{Y}_{u_k\bar{d}_1}^{H^{-*}} D_2(m_{u_j}^2, m_{u_k}^2, m_W^2, m_H^2), \\
C_2 &= \frac{-1}{32\pi^2} \frac{g^2}{m_W^2} \sum_{j,k=1}^3 V_{j2} V_{k1}^* m_d m_{u_j}^2 m_{u_k} \mathcal{Y}_{u_j\bar{d}_1}^{H^{-*}} \mathcal{Y}_{d_2\bar{u}_k}^{H^+} D_0(m_{u_j}^2, m_{u_k}^2, m_W^2, m_H^2), \\
C_2' &= \frac{-1}{32\pi^2} \frac{g^2}{m_W^2} \sum_{j,k=1}^3 V_{j1}^* V_{k2} m_s m_{u_j}^2 m_{u_k} \mathcal{Y}_{u_j\bar{d}_2}^{H^-} \mathcal{Y}_{d_1\bar{u}_k}^{H^{+*}} D_0(m_{u_j}^2, m_{u_k}^2, m_W^2, m_H^2), \\
C_4 &= \frac{-1}{32\pi^2} \frac{g^2}{m_W^2} \sum_{j,k=1}^3 \left[V_{j1}^* V_{k2} (m_{u_j} m_{u_k} m_d m_s \mathcal{Y}_{d_1\bar{u}_k}^{H^{+*}} \mathcal{Y}_{d_2\bar{u}_j}^{H^+} + m_{u_j}^2 m_{u_k}^2 \mathcal{Y}_{u_j\bar{d}_2}^{H^-} \mathcal{Y}_{u_k\bar{d}_1}^{H^{-*}}) \right. \\
&\quad \left. \times D_0(m_{u_j}^2, m_{u_k}^2, m_W^2, m_H^2) - m_W^2 V_{k1}^* V_{j2} \mathcal{Y}_{u_j\bar{d}_1}^{H^{-*}} \mathcal{Y}_{u_k\bar{d}_2}^{H^-} D_2(m_{u_j}^2, m_{u_k}^2, m_W^2, m_H^2) \right], \\
C_5 &= \frac{1}{64\pi^2} \frac{g^2}{m_W^2} \sum_{j,k=1}^3 \left(V_{j1}^* V_{k2} m_{u_j} m_s \mathcal{Y}_{d_2\bar{u}_j}^{H^+} \mathcal{Y}_{u_k\bar{d}_1}^{H^{-*}} + V_{j2} V_{k1}^* m_{u_j} m_d \mathcal{Y}_{d_1\bar{u}_j}^{H^{+*}} \mathcal{Y}_{u_k\bar{d}_2}^{H^-} \right) \\
&\quad \times D_2(m_{u_j}^2, m_{u_k}^2, m_W^2, m_H^2).
\end{aligned} \tag{3.9}$$

While for $B_{d,s} - \bar{B}_{d,s}$ the expressions above hold up to a trivial change of flavor indices, notice that to obtain the Wilson coefficients for the $D - \bar{D}$ mixing one needs to substitute $\mathcal{Y}^{H^{+*}} \leftrightarrow \mathcal{Y}^{H^-}$.

To set the constraints on the Yukawa coupling - heavy Higgs mass parameter space, we exploit the results derived by the UTFIT collaboration from the unitarity triangle analysis

generalized to the case of NP [76], where only tree-level flavor changing processes are assumed to be SM-like, while FCNC amplitudes are modified to account for generic NP effects. We use the up-to-date bounds on the $\Delta F = 2$ Wilson coefficients recently presented in [16]. We apply the constraints on the Wilson coefficients directly at a matching scale close to the EW one following the strategy in [5] (see their Table 1), barring accidental cancellations among different contributions from $\Delta F = 2$ operators.

We present the results for each generation separately by allowing only one new coupling to be non-zero for each panel presented in figure 4. Notice that the parameter ξ does not affect the strongest bounds we get from $\Delta F = 2$: unless we move far away from the $\xi \sim 0$ regime, the effect on the resulting constraints is minor. On the other hand, there is no dependence on the value of $\cos(\beta - \alpha)$ due to NP contributions involving charged Higgs states. We observe a small difference between the resulting bounds from B_d and B_s oscillations coming merely from the different CKM elements appearing in the expression for the $\Delta F = 2$ matching. The bounds in figure 4 correspond to the processes providing a constraint which limits the available parameter space in a visible manner in the plot.

3.3 Summary of flavor bounds

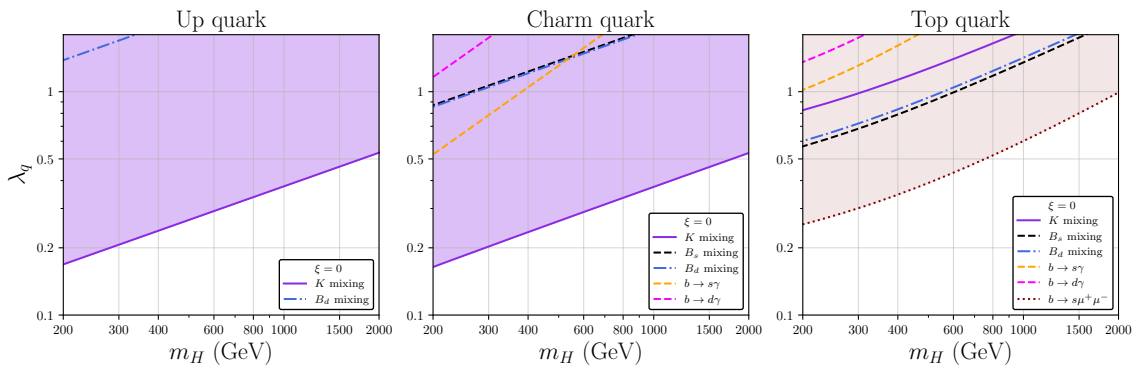


Figure 4: Bounds from FCNCs. Left Panel: Bounds on λ_u vs. m_H parameter space, setting $\xi = 0$ and $\lambda_c = \lambda_t = 0$. Middle Panel: Bounds on λ_c vs. m_H parameter space, setting $\xi = 0$ and $\lambda_u = \lambda_t = 0$. Right Panel: Bounds on λ_t vs. m_H parameter space, setting $\lambda_u = \lambda_c = 0$. These results can be sensitive to the choice of the proportionality constant ξ but are independent from different choices in the value of $\cos(\beta - \alpha)$. In the panels above, the dashed orange lines correspond to the constraints coming from the $b \rightarrow s\gamma$ decays and the dotted magenta lines to the ones from $b \rightarrow s\mu^+\mu^-$ processes. For neutral meson mixing, we only display the processes that yield a constraint for values up to $|\lambda_q| \sim 1$. We observe that for the down-type SFV 2HDM the bounds from D meson mixing are not constraining enough to limit the available parameter space in a significant way. Also, notice that $\Delta B = 2$ constraints are bounds on the absolute value of the Wilson coefficients.

We summarize here the bounds in the plane λ_q vs. m_H for the SFV down-type 2HDM. In section 3.1 and section 3.2 we present the details for the constraints we derived using the analysis of dimension-six effective operators contributing to rare B decays and

neutral meson mixing. The combined constraints are presented in [figure 4](#). In each panel of the figure we allowed only one of the new Yukawas to be non-zero, assuming the other ones to be vanishing. Notice that for all the panels of [figure 4](#) we have set $\xi = 0$, i.e. we neglected any effect of the coupling of the second Higgs doublet H_2 to the down-type quarks. Changing the value of this parameter can potentially lead to a modification of the flavor constraints shown. Also, the loop functions depend on the masses of the virtual states involved, impacting the resulting constraints. For example, in the case of $b \rightarrow s\mu^+\mu^-$, the limit of the loop function for light-quark masses leads to a suppression of the constraint observed in the top-quark panel of [figure 4](#). The differences between the constraints for the charm and up Yukawas can be attributed to the different CKM insertions that are relevant for the Wilson coefficients, as well as the size of the bounds that were used for the coefficients themselves, see [table 1](#). Notice that for the case of K mixing, the expression for C_1 when we set $\lambda_c \neq 0$ is almost identical to the one when $\lambda_u \neq 0$, because the CKM elements that appear are similar. This fact does not hold for B mixing. The constraints we get from $B_{d,s}$ for λ_u are consequently not as restrictive as they are for λ_c .

Overall, we find that the Flavor Physics constraints allow for viable parameter space where the new Yukawa couplings can be larger than their SM counterparts. For example, looking at the middle panel of [figure 4](#), we see that $|\lambda_c| \sim 0.2$ is allowed and corresponds to an enhancement of $\mathcal{Y}_{hc\bar{c}}$ about 3.7 times the SM value of y_c for $\cos(\beta - \alpha) = 0.1$.

4 Collider Direct Search Constraints

As shown in [section 3](#), flavor constraints still allow for new Higgs states with large couplings to light quarks at the EW scale. Therefore it is possible to have *direct* collider search constraints that are potentially as powerful as the precision flavor probes. In the limit of perfect alignment $\cos(\beta - \alpha) = 0$, the new heavy 2HDM states can be directly produced through both Drell-Yan production as well as quark fusion due to the large possible Yukawa couplings. Given our simplifying assumption of approximate degeneracy between H , A and H^\pm from [section 2](#), the strongest constraints come from the direct production of a single heavy Higgs state that decays into SM particles which dominate the branching fractions. In the $\cos(\beta - \alpha) = 0$ limit, while there are interesting constraints from decays exclusively into dijets [[53](#)], there is no $H - h$ mixing and therefore the Yukawa couplings of the SM are unaffected. Since we are interested in understanding the allowed parameter space for large deviations in the SM Yukawa couplings, we explore the small but non-zero $\cos(\beta - \alpha)$ limit. In this regime, as shown in [[54](#)], the decays to SM di-bosons and di-Higgs can quickly dominate the dijet branching fractions and have more sensitive cross section constraints to our underlying production mechanism in the relevant mass window. The dominant collider search constraints come from new heavy Higgs states being singly produced in quark fusion followed by decays such as $H \rightarrow ZZ$, $A \rightarrow Zh$, and $H \rightarrow hh$. For simplicity we also set the ξ parameters to 0 when investigating the direct search bounds. This does not significantly change the collider phenomenology in the regions allowed by flavor as the large *new* quark Yukawa couplings dominate direct tree-level production and the non-zero alignment parameter singles out the di-boson and di-Higgs decays in this region.

Process	Experiment	Reference	$\mathcal{L}(\text{fb}^{-1})$	Search Window [GeV]
$H \rightarrow ZZ$	ATLAS	[77]	139	[210,2000]
$H \rightarrow hh$	ATLAS CMS	[78][79][80] [81]	139 [126, 139]	[251,5000]
$A \rightarrow Zh$	ATLAS	[82]	139	[220,5000]

Table 2: Table of direct resonant searches used to constrain the model with results shown in [figure 5](#).

To determine the bounds from direct searches we use the results from resonant di-Higgs searches [78–81, 83], $A \rightarrow Zh$ [82] and $H \rightarrow ZZ$ [77], whose integrated luminosities and mass regions are summarized in [table 2](#). We recast the cross section bounds from the ATLAS and CMS searches onto our relevant parameter space by simulating the 2HDM in MADGRAPH5 [84]. We implemented a 2HDM FEYNRULES [85] file, following the SFV prescription outlined earlier. By inputting this model into MADGRAPH5 [84], we were able to scan over the relevant $\lambda_q - m_H$ parameter space for a fixed $\cos(\beta - \alpha)$ to find the direct search constraints. Given that we are interested in how charming the Higgs can be, as well as the novel enhancement of the up-quark Yukawa, we present the results for $\lambda_c - m_H$ and $\lambda_u - m_H$ for $\cos(\beta - \alpha) = 0.1$ in panels (a) and (b) of [figure 5](#). From this figure we also see that the direct search constraints are currently stronger than the flavor bounds *despite* having a non MFV texture and EW scale Higgs masses. This emphasizes the power of flavor changing suppression in SFV scenarios as well as the strength of the LHC to directly probe these flavorful states at the EW to TeV scale. On the right hand axis we also show the modification to the appropriate SM Higgs Yukawa coupling κ_{q_i} for the given input parameters of the model. In panels (b) and (c) of [figure 5](#) we show the same parameter space constraints, but for $\cos(\beta - \alpha) = 0.05$. This demonstrates how the κ_{q_i} parameter shifts accordingly, but also slight changes in the direct search constraints due to the dependence of the di-boson couplings on the alignment parameter. Note, however that the new Yukawa coupling is unaffected in the small alignment parameter limit. In all panels of [figure 5](#) we see that the bounds on λ_u are stronger than those on λ_c due to the enhanced PDFs of the up quark compared to the charm quark. However interpreted in terms of the κ_{q_i} they are very different due to the underlying SM Yukawa coupling predictions.

5 Higgs precision and Yukawa Coupling measurements

We are now in a position to attempt to answer our titular question. As shown in [section 3](#) and [section 4](#), flavor and direct search collider constraints place strong bounds on a down-type SFV 2HDM model. However, as demonstrated, there is still the possibility that these models can generate large deviations in the up and charm SM Higgs Yukawa couplings.

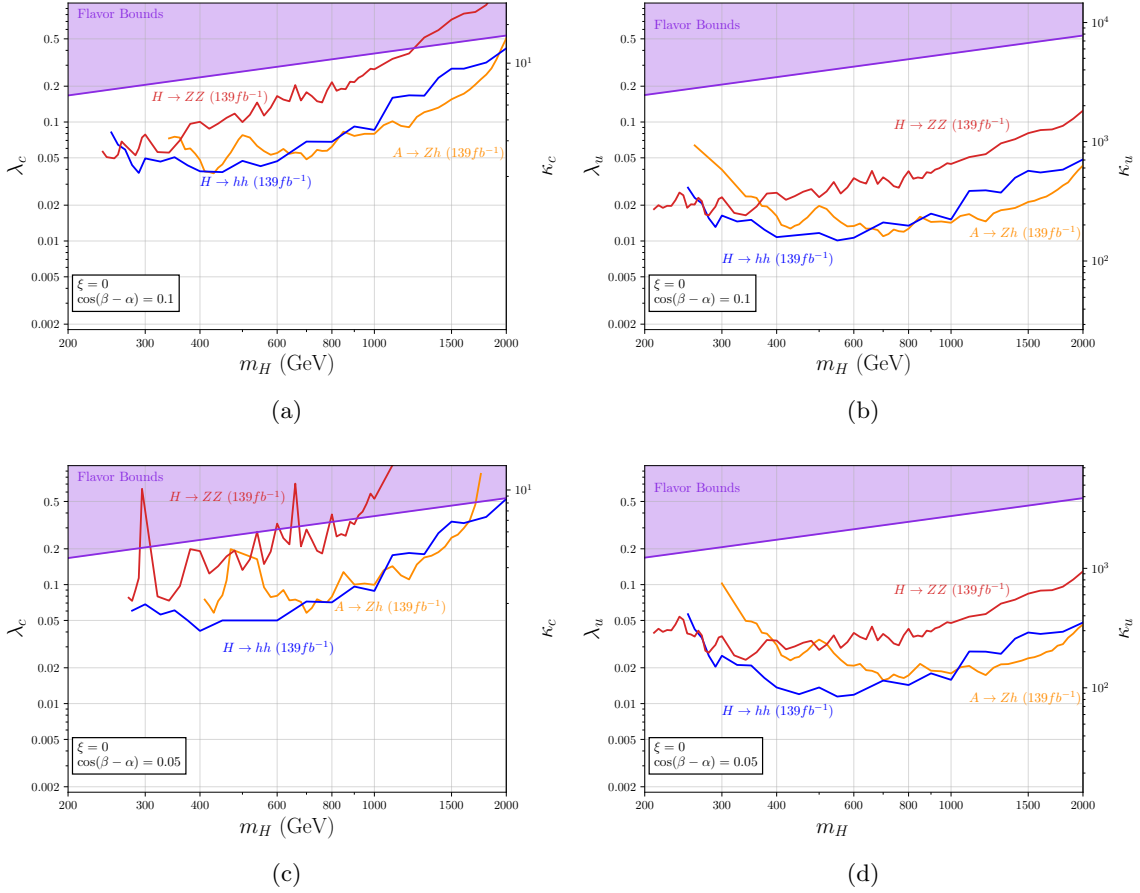


Figure 5: Collider searches for the 2HDM model with couplings to charm in panel (a) and up in quarks panel (b), overlaid with the appropriate flavor bounds derived in section 3. The couplings of the second doublet to the down-type quarks are set to zero i.e. $\xi = 0$ and the alignment parameter is set to $\cos(\beta - \alpha) = 0.1$. The vertical axis on the right-hand side of each panel shows the coupling modifier of the charm and up quarks respectively. The combined flavor bounds are presented in purple. We present the bounds of resonant production of the heavy Higgs H , decaying to different channels. The bounds from decays to a pair of Z bosons [77] are in red and to a pair of 125 GeV Higgs [78–80] are in blue. In orange, we present the bounds from resonant production of the CP odd A decaying to a Z boson and a 125 GeV Higgs boson [82]. Panels (c) and (d) are the same as (a) and (b) with $\cos(\beta - \alpha) = 0.05$.

Therefore it is important to correlate with the precision measurements of the SM Higgs couplings to understand how complementary these measurements are.

A common approach for single-Higgs precision at the LHC is based on exclusive final states that are correlated with a production mechanism for the Higgs and reported as signal

strength modifiers:

$$\mu_{if} = \frac{\sigma_i \times \text{BF}_f}{\sigma_i^{\text{SM}} \times \text{BF}_f^{\text{SM}}}. \quad (5.1)$$

Large modifications of light quark Yukawas due to our 2HDM can affect the signal strengths in a number of ways. First, if there is mixing between the heavy and light Higgs states to generate Yukawa coupling modifications there is an inherent dilution of SM Higgs couplings. Second, in the limit of a large Yukawa modification, the branching fractions to *all* exclusive final states will be modified which can be correlated across production mechanisms since the total width changes as

$$\frac{\Gamma_{tot}^{\text{SM}}}{\Gamma_{tot}} = \left[\sin^2(\beta - \alpha) \left(1 + \frac{\Gamma_{qq}^{\text{SM}}}{\Gamma_{tot}^{\text{SM}}} \left(\frac{\lambda_q^2}{\sin^2(\beta - \alpha)y_q^2} - 1 \right) \right) \right]^{-1}. \quad (5.2)$$

A correlated effect, but subleading for most measurements, is the modification of the production cross section both in terms of loop effects as well as enhancing additional production modes. Finally, if a light quark Yukawa coupling is large enough, it is possible for the statistics to be sufficient for a direct measurement via flavor tagging. The effects can be quantified through Higgs coupling modifier fits with κ_{q_i} or in an EFT framework. Given that we have the full 2HDM model it is more straightforward to use coupling modifiers to correlate across observables. The explicit dependence on the model parameters for κ_{q_i} defined in Eq. (2.11) can be found in Appendix C. For the first two effects on Higgs precision there is no measurement of the modified Yukawa coupling “directly”, therefore the bounds they provide on the up and charm Yukawa couplings are less robust to other possible BSM effects. Nevertheless, in the context of the specific model we study, they give constraints on both κ_c and κ_u that we refer to as normalization constraints. As mentioned in section 1, one can go beyond signal strengths and include differential shape effects in the p_T spectrum, but these represent marginal improvements currently. When the coupling modifier is large enough, additional production modes, exclusive decays and flavor tagging can provide measurements that are easier to directly correlate with the change in the light quark Yukawa couplings. However, these bounds are typically much weaker, and only promising at the LHC for modifications of the charm Yukawa coupling.

In table 3 we present all the single-Higgs precision studies relevant for the modification of light quark Yukawas that we use in this study. We give results of the studies as a single modifier of the charm Yukawa coupling, κ_c to give an overview of the sensitivity of all charm related measurements performed thus far. These results are not being combined, but only serve to illustrate the sensitivity to individual methods. In most cases the experiments have made the κ_c interpretation themselves, but for the “normalization” of the best measured exclusive channels we have recast this ourselves, *assuming* a central value of the SM prediction and *only* a modification of the branching fractions. The purpose of this is to give an understanding of how constraining non-charm final states are given their high precision, even though they are a more indirect constraint. We have also recast the exclusive final state $h \rightarrow J/\psi Z$ from [32] using the results of [86] as this was reported only

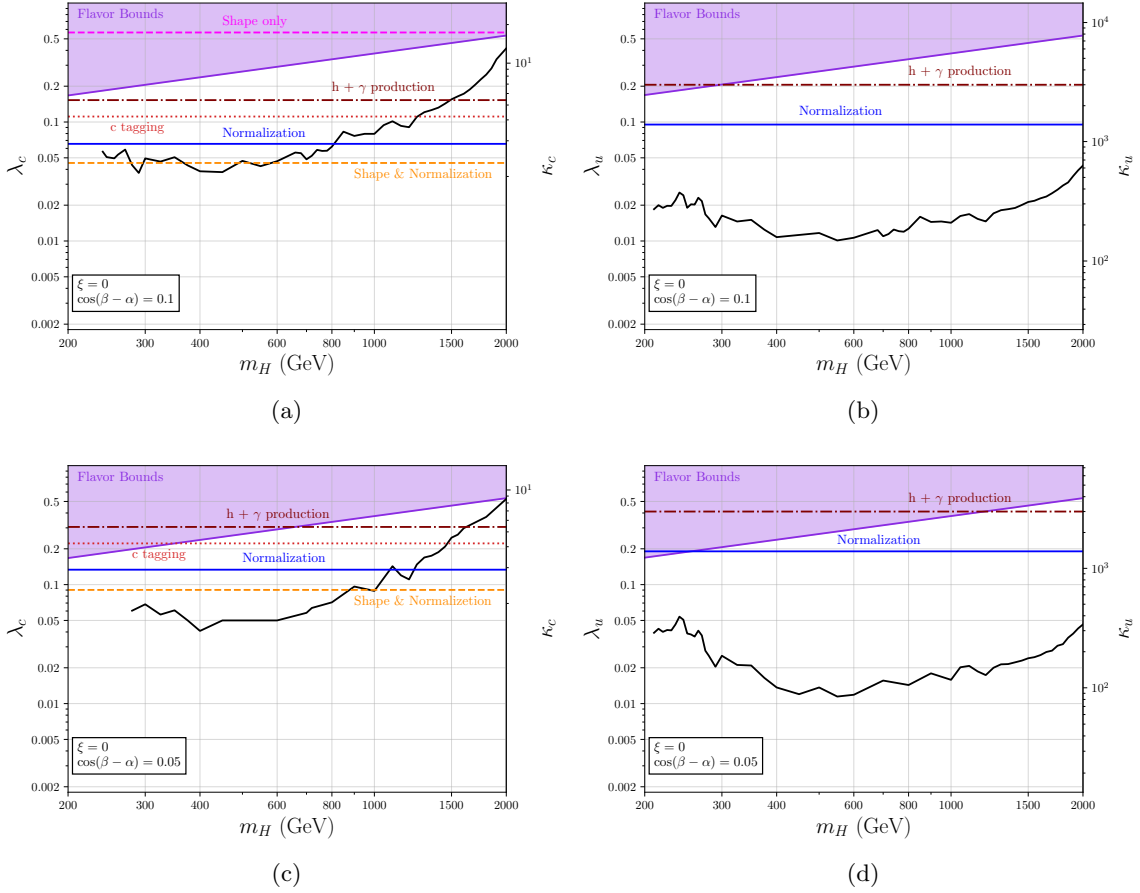


Figure 6: We present the constraints for the new Yukawa couplings of our 2HDM model derived using single-Higgs properties as measured at the LHC at 95 % C.L. The combined constraints from resonant decays of the Higgs from [figure 5](#) are shown in black and overlaid with the flavor bounds from [section 3](#). Panel (a): Constraints of the new charm Yukawa coupling. The solid blue line shows the bounds from the Higgs signal modifier for the $\mu^{\gamma\gamma}$ channel [22] assuming that the central value is the SM i.e. $\mu^{\gamma\gamma} = 1$. The dotted red lines correspond to the constraint obtained by c-tagging searches [30]. The dashed orange line corresponds to constraints using both shape and normalization of κ_c derived from p_t measurements [27]. When compared to the blue normalization line, this shows that normalization dominates the results. The maroon dotted dashed line corresponds to constraints from $h + \gamma$ production [29]. Panel (b): Constraints on the modified up Yukawa coupling. The combined constraints from resonant decays of the Higgs eigenstates from [figure 5](#) are shown in black. The solid blue line corresponds to the bounds derived from the Higgs signal modifier for the $\mu^{\gamma\gamma}$ channel [22]. The maroon dotted dashed line corresponds to constraints from $h\gamma$ production [29]. Panels (c) and (d) are the same as (a) and (b) respectively but for $\cos(\beta - \alpha) = 0.05$.

as an upper limit on the branching fraction by CMS. All the normalization bounds can

also be recast trivially for a κ_u only modification as well. However, charm tagging of the Higgs or other associated final states cannot be recast for κ_u . One can also tag or look for exclusive mesonic decays into the first generation, and in some cases we note where an experiment has performed this study and interpretation. However, the projected bounds on κ_u are weaker than existing flavor and direct constraints and therefore not relevant at the LHC or HL-LHC for this class of models.

Experiment	Reference	$\mathcal{L}(fb^{-1})$	Constraints	Comments
ATLAS	[22]	139	$ \kappa_c < 2.91$	Normalization
CMS	[25]	138	$ \kappa_c < 2.92$	Normalization
ATLAS	[28]	139	$\kappa_c \in (-2.27, 2.27)$ $\kappa_c \in (-8.6, 17.3)$	(p_T measurement, Shape & Normalization) p_T measurement, Shape only
CMS	[29]	138	$\kappa_c \in (-6, 5.4)$	$h + \gamma$ associated production
CMS	[23]	138	$1.1 < \kappa_c < 5.5$	c-tagging
ATLAS	[30]	140	$ \kappa_c < 4.2$	c-tagging
CMS	[31]	138	$ \kappa_c < 38.1$	$h + c$ associated production
ATLAS	[21]	139	$\kappa_c/\kappa_\gamma \in (-153, 175)$	$h \rightarrow J/\psi\gamma$ decays
CMS	[32]	138	$\kappa_c \in (-7.5 \times 10^3, 7.7 \times 10^3)$	$h \rightarrow J/\psi Z$ decays

Table 3: Table of Higgs precision results, note that the results quoted in this table correspond to 95 % C.L. and are recast as bounds on the charm quark coupling modifier. In cases where the experimental result does not include an interpretation in terms of κ_c we mark with an asterisk and refer to the text. Using the normalization measurements we can place similar bounds for the up quark as well. Note also that in reference [29] there is an explicit translation of their results into coupling modifier language, getting $\kappa_u \in [-3, 3] \times 10^3$ at 95 % C.L. For the case of [22, 25], in order to translate the signal modifier constraint $\mu^{\gamma\gamma}$ to the charm coupling modifier presented in this table, we assume that the only modification to the SM couplings is the one for the charm Yukawa and that the production cross section does not get modified. For both cases we center the measurements at the SM prediction namely $\mu^{\gamma\gamma} = 1$. Finally, for the case of [32], we use the expression in [86] to extract the constraint presented on the table. Notice that ATLAS has also recently studied associated production of charm and Higgs inclusively, providing a bound with no κ_c -tagging [33].

In panels (a) and (b) of figure 6 we present the results of the flavor and direct searches from the previous sections overlaid with the constraints from the single-Higgs precision results given in table 3 for an alignment parameter of $\cos(\beta - \alpha) = 0.1$. In panel (a) of figure 6, the results for how charming the SM Higgs can be are shown. Note that there is strong complementarity between the flavor, direct collider search, and precision single-Higgs results. In particular, for $m_H \lesssim 300$ GeV and $m_H \gtrsim 1.2$ TeV, the Higgs signal strength normalization constraints are the strongest, while in the intermediate regime the direct

searches provide the strongest bounds on the charm Yukawa coupling. It is interesting to note that while charm tagging is currently a weaker bound than normalization, in the large mass regime it still provides constraints beyond the direct collider searches. Therefore in an extension of this model where the normalization bound is ameliorated, it would be possible for charm tagging to provide valuable new information compared to other constraints. Additionally, since charm tagging has room for substantial improvement based on methodology not just statistics, the fact that there is parameter space that is *already* sensitive beyond other observables, gives strong motivation to continue improving charm tagging performance. In panel (b) of [figure 6](#), we see the analogous constraints on κ_u . There is an important distinction compared to κ_c , in all regions of parameter space the di-boson and di-Higgs searches provide the strongest constraint compared to Higgs precision. Therefore for the foreseeable future, the strongest bounds on first generation quark Yukawas don't come from Higgs precision or flavor, but by searching for the flavored progenitors at high energy.

To help illustrate the behavior for smaller values of the alignment parameter, we show the same parameter space as [figure 6](#) panels (a) and (b) but for $\cos(\beta - \alpha) = 0.05$ in panels (c) and (d) of [figure 6](#). Note that roughly the same conclusions can be drawn for all panels of [figure 6](#) but the single-Higgs precision bounds are weaker due to the smaller alignment parameter for panels (c) and (d).

Finally, to understand more generally the interplay with precision Higgs constraints, we show the allowed region as function of the new Yukawa couplings λ_u and λ_c and $\cos(\beta - \alpha)$ in [figure 7](#). We also plot contours of constant κ_u and κ_c to demonstrate the large deviations possible even at extremely small values of $\cos(\beta - \alpha)$.

6 Conclusions

In this work we have focused on the phenomenology of a 2HDM realizing down-type Spontaneous Flavor Violation (SFV). This allowed for a concrete realization of models which could significantly modify the *charm* and/or *up* quark Yukawa couplings of the SM Higgs while maintaining consistency with all precision flavor experiments.

In particular, we have demonstrated that flavor constraints can allow for a second Higgs with Yukawa couplings of $\mathcal{O}(10^{-1})$ to any up-type quark *without* having to respect any of the hierarchies of the SM Yukawas. For example one could have a new Higgs that couples at this strength *only* to the charm quark. When this new Higgs has a non-zero mixing with the SM Higgs, this allows for large deviations of $\mathcal{O}(10)$ to $\mathcal{O}(10^4)$ to the SM charm and up Yukawa couplings consistent with measurements of FCNCs.

Flavor constraints are not the only relevant constraints for a new state near the EW scale with potentially large couplings to light quarks. Direct search constraints are particularly powerful given that if there is mixing between the SM Higgs and heavier Higgs this implies that the heavier Higgs can decay into di-bosons and di-Higgs. We find that these direct search constraints are always stronger than flavor bounds in the limit of small but non-zero mixing for the down-type SFV 2HDM cases we explored.

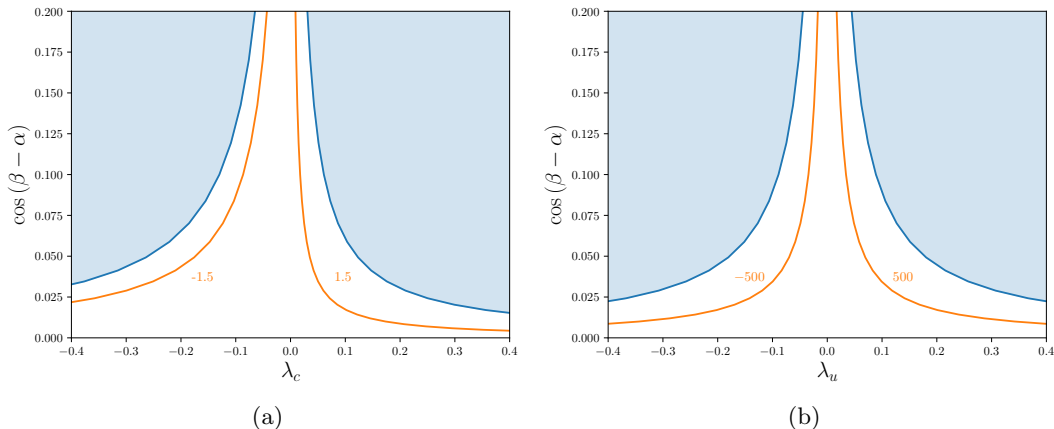


Figure 7: Constraints on the allowed values of the $\lambda_c - \cos(\beta - \alpha)$. In order to derive these constraints we use the signal modifier $\mu_{ggF}^{\gamma\gamma}$ from [22]. Assuming that only λ_q is non-zero, with $q = c$ for the left panel and $q = u$ for the right one, we can extract limits for the coupling modifier κ_{q_i} at 95 % C.L. which we can then recast in the parameter space of our model, shown as the shaded blue region. Note that for the $\mu_{ggF}^{\gamma\gamma}$ to κ_{q_i} conversion, we also assume that the production cross sections do not change from their SM values. For the case of λ_u the results are almost symmetric around $\lambda_u = 0$ because κ_u is significantly less constraint compared to κ_c and dominates the expression. Finally, in order to make comparison with the SM easier, we present the contour lines for $\kappa_u = \pm 500$ and $\kappa_c = \pm 1.5$ within the model.

Finally, we examined whether or not the allowed parameter space was consistent with the Higgs precision measurements. The strongest constraints from single-Higgs precision currently come from the best measured exclusive channels. However, we have shown that the direct search constraints for the new Higgs states which could cause measurable SM Higgs deviations are generically more powerful at the LHC. At very low or high masses of the second Higgs state the indirect single-Higgs precision constraints are stronger for charm Yukawa deviations, while for the up-quark case we found direct search constraints and flavor are always stronger. We have also updated the up-type SFV 2HDM bounds from [54] in Appendix A, which reaches a similar conclusion. While indirect single-Higgs precision constraints are powerful, what is more exciting is the possibility of improvements in direct charm-tagging measurements at the LHC and beyond in light of the extraordinary advancement provided by machine learning in High Energy. We have demonstrated that there are viable models consistent with flavor and direct searches that could be explored in a new way with improvements in charm tagging. This is of particular significance as current projections require an $\mathcal{O}(1)$ deviation in the charm Yukawa for LHC sensitivity which is difficult to account for in standard flavor models.

Finally it is important to remember that in the pursuit of how charming the Higgs can be, as well as the deviations in other light quark Yukawas, it is always tied to the UV model. While there could be large deviations as no one has any idea of the origin of

flavor in our universe, there still must be a mechanism to explain significant deviations in while maintaining consistency with experimental results. For any light quark Yukawa deviation that is sizable enough to be relevant at the LHC, the scale of new physics cannot be parametrically separated from the EW scale without running into unitarity bounds. Therefore any observables attempting to test Yukawa couplings in the SM must be compared to other data which explores possible UV completions, of which few are currently known. Therefore the LHC is currently ideally suited to carry out this program of both precision and energy frontier measurements. Furthermore, a future high energy e^+e^- linear collider, proton collider or muon collider at the 10 TeV pcm scale would likely be able to cover the entire parameter space of known UV origins for measurable light quark Yukawa coupling deviations. We leave investigating these options and the larger parameter space that could be explored within SFV 2HDMs for future work.

Acknowledgments

We would like to thank Hannah Arnold, Livia Soffi and Samuel Homiller for useful discussions and feedback. M.V. acknowledges support from the projects ‘‘Exploring New Physics’’ and ‘‘Theoretical Particle Physics and Cosmology’’ funded by INFN and thanks YITP and SCGP for the hospitality during the completion of the work. The work of A.S.G. and P.M is supported in part by the National Science Foundation grant PHY-2210533.

A 2HDM: The up-type SFV case

In this section we present the constraints we get following the up-type SFV flavor prescription for a 2HDM, updating the ones set in [53]. The new results we present here are produced using new constraints on dimension-six operators and LHC data from Run 2, see references in [table 1](#) and [table 2](#). In order to make the comparison with [53] straightforward, we make the same choice for ξ and the alignment parameter $\cos(\beta - \alpha)$ for the flavor and collider bounds respectively. As we saw in [section 2](#), within the SFV prescription, only one quark sector can be aligned. For the up-type SFV 2HDM, the new Yukawa couplings will appear in the down quark sector and the couplings for the second Higgs doublet will have the following form,

$$\mathcal{Y}_2^u = \xi V^* Y^u, \quad \mathcal{Y}_2^d = -\text{diag}(\lambda_d, \lambda_s, \lambda_b), \quad \mathcal{Y}_2^\ell = -\xi^\ell Y^\ell. \quad (\text{A.1})$$

Similar to the case for the down-type SFV prescription, the same parameters ξ and ξ^ℓ control the coupling strength of the second doublet to the up-type quarks and the leptons, respectively. As expected, our flavor bounds will depend on the values of these two parameters. In accordance with the rest of this work, we will set $\xi^\ell = 0$, concentrating our attention on the quark sector. Below we present the bounds derived using recent results from Flavor Physics for the allowed values of the relevant Wilson coefficients, see [table 1](#). The functional dependence of the Wilson coefficients to the up-type SFV model parameters can be derived using the same expressions mentioned in [section 3](#) and the up-type couplings in the Appendix of [53]. Note that the resulting dependence of the coefficients on the 2HDM

parameters will be different than the one for the down-type prescription. We can verify this by comparing the expressions for the up-type couplings in equation (A.1) with the equivalent ones in the down-type case listed in Appendix C.

By comparing the results in the first row of figure 8, where we have set $\xi = 0.1$, with the ones in the second row of the same figure, where $\xi = 1$, we can verify that the Flavor Physics constraints are sensitive to the value of ξ . This behavior is the result of the explicit dependence of the Wilson coefficients on the NP parameters. Overall, the ability to place bounds on the parameter space of our 2HDM depends on the flavor prescription that we follow (up or down-type SFV) and the specific value we choose for ξ . This sensitivity depends on which quark sector contains the new couplings. With the SFV prescription we can only produce new aligned couplings for either the up or down quarks. Finally, we note that as is the case for down-type SFV, the Flavor Physics bounds for the up-type SFV 2HDM do not depend on the alignment parameter because the Higgs eigenstates involved in these processes are the charged ones. Finally, using MADGRAPH [84] we recast experimental bounds from collider searches in the up-type SFV model parameter space. As we did in section 4, we concentrate on the quark sector by setting the couplings to the leptons to zero, $\xi^\ell = 0$. We choose to consider a regime away from alignment, $\cos(\beta - \alpha) \neq 0$. As a result, setting $\xi = 0$ does not prevent the modification of all the 125 GeV Higgs Yukawa couplings. The results are presented in figure 9, showing the same search channels as in figure 5 for the down-type SFV.

B Loop functions

The loop functions used in the previous sections are defined as follows [66, 74]:

$$\begin{aligned}
\mathcal{C}_{7,XY}^0(z_j) &= \frac{z_j}{12} \left[\frac{-5z_j^2 + 8z_j - 3 + (6z_j - 4) \log z_j}{(z_j - 1)^3} \right], \\
\mathcal{C}_{8,XY}^0(z_j) &= \frac{z_j}{4} \left[\frac{-z_j^2 + 4z_j - 3 - 2 \log z_j}{(z_j - 1)^3} \right], \\
\mathcal{C}_{7,YY}^0(z_j) &= \frac{z_j}{72} \left[\frac{-8z_j^3 + 3z_j^2 + 12z_j - 7 + (18z_j^2 - 12z_j) \log z_j}{(z_j - 1)^4} \right], \\
\mathcal{C}_{8,YY}^0(z_j) &= \frac{z_j}{24} \left[\frac{-z_j^3 + 6z_j^2 - 3z_j - 2 - 6z_j \log z_j}{(z_j - 1)^4} \right], \\
I_1(z_j) &= -\frac{1}{z_j - 1} + \frac{\log(z_j)z_j}{(z_j - 1)^2}.
\end{aligned}$$

With $d = 4 - 2\epsilon$, we get for the loop functions appearing in the box diagram calculations in eqs. (3.9) and (3.8):

$$\begin{aligned} \mathcal{C}_0(m_1^2, m_2^2, m_3^2) &= \frac{m_1^2 m_2^2 \log\left(\frac{m_1^2}{m_2^2}\right) + m_3^2 m_2^2 \log\left(\frac{m_2^2}{m_3^2}\right) + m_3^2 m_1^2 \log\left(\frac{m_3^2}{m_1^2}\right)}{(m_1^2 - m_2^2)(m_3^2 - m_1^2)(m_2^2 - m_3^2)}, \\ D_0(m_1^2, m_2^2, m_3^2, m_4^2) &= \frac{\mathcal{C}_0(m_1^2, m_2^2, m_3^2) - \mathcal{C}_0(m_1^2, m_2^2, m_4^2)}{m_3^2 - m_4^2}, \\ D_2(m_1^2, m_2^2, m_3^2, m_4^2) &= \mathcal{C}_0(m_1^2, m_2^2, m_3^2) + m_4^2 D_0(m_1^2, m_2^2, m_3^2, m_4^2). \end{aligned}$$

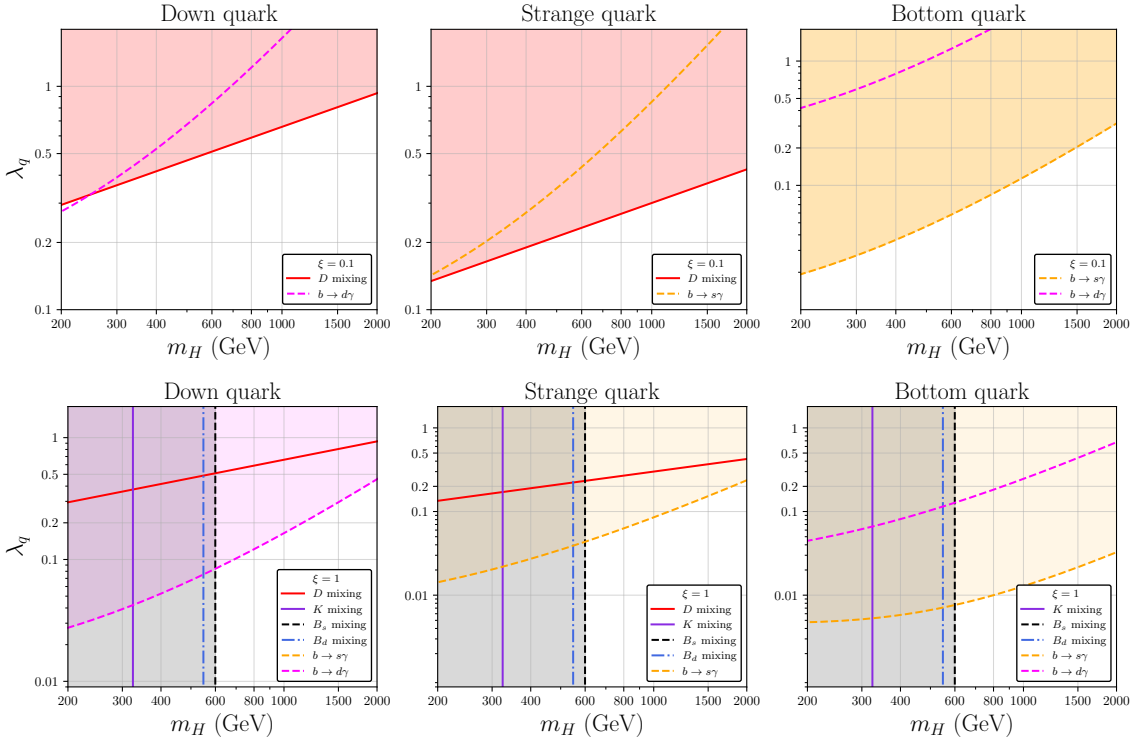


Figure 8: Bounds from FCNCs for the up-type SFV. The top row shows bounds for different couplings λ_{q_i} with $\xi = 0.1$: (left) λ_d with $\lambda_s = \lambda_b = 0$; (middle) λ_s with $\lambda_d = \lambda_b = 0$; (right) λ_b with $\lambda_d = \lambda_s = 0$. The bottom row presents the same bounds for $\xi = 1$. The value of $\cos(\beta - \alpha)$ does not affect these results since only the charged Higgs eigenstates are involved in these processes. Due to the different structure of the Yukawa matrices for the up-type SFV, we see that bounds coming from D meson mixing now become much stricter compared to the down-type SFV case shown in figure 4. We present in solid red lines the constraints coming from D meson mixing and in dashed orange and magenta lines the ones coming from $b \rightarrow s\gamma$ and $b \rightarrow d\gamma$ decays respectively. The bounds of the relevant effective operators are shown in table 1. Notice that the flavor bounds depend strongly on the value of ξ that we choose.

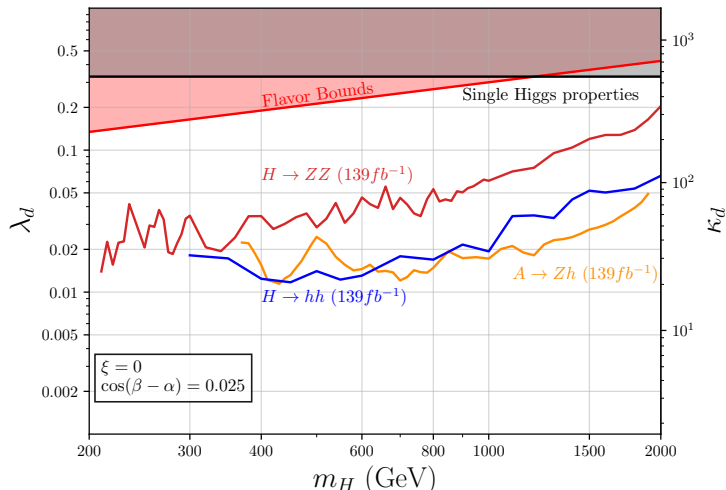


Figure 9: Collider searches for the 2HDM model with couplings to down-type quarks, overlaid with the flavor bounds for $\xi = 0$. The couplings of the second doublet to the up-type quarks are set to zero i.e. $\xi = 0$ and the alignment parameters is set to $\cos(\beta - \alpha) = 0.025$. The vertical axis on the right hand side shows the enhancement of the coupling of h to the down quarks with respect to the Standard Model Yukawa. The flavor bounds combined are presented in light red. We present the bounds of resonant production of the heavy Higgs H , decaying to different channels. The bounds from decays to a pair of Z bosons [77] are in red and to a pair of 125 GeV Higgs [78–80] are in blue. In orange, we present the bounds from resonant production of the CP odd A decaying to a Z boson and a 125 GeV Higgs boson [82]. Finally, in black we present the bound that we obtain from the Higgs signal modifier [22, 25].

C Couplings in down-type SFV

In table 4 we show the physical couplings of the Higgs eigenstates to the fermions derived from Eq. (2.3) for the down-type SFV case. In order to keep the notation as clear as possible, in the table we denote by bar the right handed fields. We denote by Y^q with $q = u, d, \ell$ the Standard Model Yukawa matrices for up, down-type quarks and leptons respectively. $\Lambda^u = \text{diag}(\lambda_u, \lambda_c, \lambda_t)$ is the diagonal matrix containing the three new couplings introduced in the down-type SFV 2HDM. Couplings are defined with a negative sign in the Lagrangian, i.e. $\mathcal{L} \supset -\lambda_{hf\bar{f}} h f \bar{f}$.

References

- [1] UTFIT Collaboration, M. Bona et al., *Model-independent constraints on $\Delta F = 2$ operators and the scale of new physics*, *JHEP* **03** (2008) 049, [[arXiv:0707.0636](#)].
- [2] G. Isidori, Y. Nir and G. Perez, *Flavor Physics Constraints for Physics Beyond the Standard Model*, *Ann. Rev. Nucl. Part. Sci.* **60** (2010) 355, [[arXiv:1002.0900](#)].

$\mathcal{Y}_{u_i \bar{u}_j}^h$	$\delta_{ij} [Y_i^u \sin(\beta - \alpha) + \Lambda_i^u \cos(\beta - \alpha)]$	$\mathcal{Y}_{u_i \bar{u}_j}^H$	$\delta_{ij} [-Y_i^u \cos(\beta - \alpha) + \Lambda_i^u \sin(\beta - \alpha)]$
$\mathcal{Y}_{d_i \bar{d}_j}^h$	$\delta_{ij} Y_i^d [\sin(\beta - \alpha) + \xi \cos(\beta - \alpha)]$	$\mathcal{Y}_{d_i \bar{d}_j}^H$	$\delta_{ij} Y_i^d [-\cos(\beta - \alpha) + \xi \sin(\beta - \alpha)]$
$\mathcal{Y}_{\ell_i \bar{\ell}_j}^h$	$\delta_{ij} Y_i^\ell [\sin(\beta - \alpha) + \xi^\ell \cos(\beta - \alpha)]$	$\mathcal{Y}_{\ell_i \bar{\ell}_j}^H$	$\delta_{ij} Y_i^\ell [-\cos(\beta - \alpha) + \xi^\ell \sin(\beta - \alpha)]$
$\mathcal{Y}_{u_i \bar{u}_j}^A$	$i\delta_{ij} \Lambda_i^u$	$\mathcal{Y}_{d_i \bar{u}_j}^{H^+}$	$(V^T \Lambda^u)_{ij}$
$\mathcal{Y}_{d_i \bar{d}_j}^A$	$-i\xi \delta_{ij} Y_i^d$	$\mathcal{Y}_{u_i \bar{d}_j}^{H^-}$	$-(\xi V^* Y^d)_{ij}$
$\mathcal{Y}_{\ell_i \bar{\ell}_j}^A$	$-i\xi^\ell \delta_{ij} Y_i^\ell$	$\mathcal{Y}_{\ell_i \bar{\ell}_j}^{H^-}$	$-(\xi^\ell Y^\ell)_{ij}$

Table 4: Higgs couplings to the fermions in the mass basis, see the text for details.

- [3] A. J. Buras, P. Gambino, M. Gorbahn, S. Jager and L. Silvestrini, *Universal unitarity triangle and physics beyond the standard model*, *Phys. Lett. B* **500** (2001) 161–167, [[arXiv:hep-ph/0007085](#)].
- [4] G. D’Ambrosio, G. F. Giudice, G. Isidori and A. Strumia, *Minimal flavor violation: An Effective field theory approach*, *Nucl. Phys. B* **645** (2002) 155–187, [[arXiv:hep-ph/0207036](#)].
- [5] L. Silvestrini and M. Valli, *Model-independent Bounds on the Standard Model Effective Theory from Flavour Physics*, *Phys. Lett. B* **799** (2019) 135062, [[arXiv:1812.10913](#)].
- [6] J. Aebischer, C. Bobeth, A. J. Buras and J. Kumar, *SMEFT ATLAS of $\Delta F = 2$ transitions*, *JHEP* **12** (2020) 187, [[arXiv:2009.07276](#)].
- [7] R. Aoude, T. Hurth, S. Renner and W. Shepherd, *The impact of flavour data on global fits of the MFV SMEFT*, *JHEP* **12** (2020) 113, [[arXiv:2003.05432](#)].
- [8] C. Grunwald, G. Hiller, K. Kröninger and L. Nollen, *More synergies from beauty, top, Z and Drell-Yan measurements in SMEFT*, *JHEP* **11** (2023) 110, [[arXiv:2304.12837](#)].
- [9] A. Greljo and A. Palavrić, *Leading directions in the SMEFT*, *JHEP* **09** (2023) 009, [[arXiv:2305.08898](#)].
- [10] F. Garosi, D. Marzocca, A. R. Sánchez and A. Stanzione, *Indirect constraints on top quark operators from a global SMEFT analysis*, *JHEP* **12** (2023) 129, [[arXiv:2310.00047](#)].
- [11] L. Allwicher, C. Cornella, G. Isidori and B. A. Stefanek, *New physics in the third generation. A comprehensive SMEFT analysis and future prospects*, *JHEP* **03** (2024) 049, [[arXiv:2311.00020](#)].
- [12] R. Bartocci, A. Biekötter and T. Hurth, *A global analysis of the SMEFT under the minimal MFV assumption*, [arXiv:2311.04963](#).
- [13] G. Isidori and S. Trifinopoulos, *Exploring the flavour structure of the high-scale MSSM*, *Eur. Phys. J. C* **80** (2020) 291, [[arXiv:1912.09940](#)].
- [14] W. Altmannshofer and J. Zupan, *Snowmass White Paper: Flavor Model Building*, in *Snowmass 2021*, 3, 2022. [arXiv:2203.07726](#).
- [15] A. Glioti, R. Rattazzi, L. Ricci and L. Vecchi, *Exploring the Flavor Symmetry Landscape*, [arXiv:2402.09503](#).
- [16] M. Bona, M. Ciuchini, D. Derkach, R. Di Palma, F. Ferrari, V. Lubicz et al., *Overview and theoretical prospects for CKM matrix and CP violation from the UTfit Collaboration*, *PoS WIFAI2023* (2024) 007.
- [17] G. F. Giudice, *The Dawn of the Post-Naturalness Era*, pp. 267–292. 2019. [arXiv:1710.07663](#).

- [18] N. Craig, *Naturalness: past, present, and future*, *Eur. Phys. J. C* **83** (2023) 825, [[arXiv:2205.05708](#)].
- [19] S. Dawson et al., *Report of the Topical Group on Higgs Physics for Snowmass 2021: The Case for Precision Higgs Physics*, in *Snowmass 2021*, 9, 2022. [[arXiv:2209.07510](#)].
- [20] ATLAS Collaboration, *Direct constraint on the Higgs-charm coupling from a search for Higgs boson decays into charm quarks with the ATLAS detector*, *Eur. Phys. J. C* **82** (2022) 717, [[arXiv:2201.11428](#)].
- [21] ATLAS Collaboration, *Searches for exclusive Higgs and Z boson decays into a vector quarkonium state and a photon using 139 fb^{-1} of ATLAS $\sqrt{s} = 13 \text{ TeV}$ proton-proton collision data*, *Eur. Phys. J. C* **83** (2023) 781, [[arXiv:2208.03122](#)].
- [22] ATLAS Collaboration, *A detailed map of Higgs boson interactions by the ATLAS experiment ten years after the discovery*, *Nature* **607** (2022) 52–59, [[arXiv:2207.00092](#)].
- [23] CMS Collaboration, *Search for Higgs Boson Decay to a Charm Quark-Antiquark Pair in Proton-Proton Collisions at $s=13 \text{ TeV}$* , *Phys. Rev. Lett.* **131** (2023) 061801, [[arXiv:2205.05550](#)].
- [24] CMS Collaboration, *A search for the standard model Higgs boson decaying to charm quarks*, *JHEP* **03** (2020) 131, [[arXiv:1912.01662](#)].
- [25] CMS Collaboration, *A portrait of the Higgs boson by the CMS experiment ten years after the discovery.*, *Nature* **607** (2022) 60–68, [[arXiv:2207.00043](#)].
- [26] ATLAS Collaboration, *Searches for exclusive Higgs and Z boson decays into $J/\psi\gamma$, $\psi(2S)\gamma$, and $\Upsilon(nS)\gamma$ at $\sqrt{s} = 13 \text{ TeV}$ with the ATLAS detector*, *Phys. Lett. B* **786** (2018) 134–155, [[arXiv:1807.00802](#)].
- [27] ATLAS Collaboration, *Measurements of the Higgs boson inclusive and differential fiducial cross-sections in the diphoton decay channel with pp collisions at $\sqrt{s} = 13 \text{ TeV}$ with the ATLAS detector*, *JHEP* **08** (2022) 027, [[arXiv:2202.00487](#)].
- [28] ATLAS Collaboration, *Measurement of the total and differential Higgs boson production cross-sections at $\sqrt{s} = 13 \text{ TeV}$ with the ATLAS detector by combining the $H \rightarrow ZZ^* \rightarrow 4\ell$ and $H \rightarrow \gamma\gamma$ decay channels*, *JHEP* **05** (2023) 028, [[arXiv:2207.08615](#)].
- [29] CMS Collaboration, *Search for γH production in pp collisions at $\sqrt{s} = 13$ and constraints on the Yukawa couplings of light quarks to the Higgs boson using data from the CMS detector*, tech. rep., CERN, Geneva, 2024 <https://cds.cern.ch/record/2911152>.
- [30] ATLAS Collaboration, *Measurements of WH and ZH Higgs production with decays into bottom quarks and direct constraints on the charm Yukawa coupling with 13 TeV collisions in the ATLAS detector.*, tech. rep., CERN, Geneva, 2024 <https://cds.cern.ch/record/2905263>.
- [31] CMS Collaboration, *Search for Higgs boson production in association with a charm quark in the diphoton decay channel*, tech. rep., CERN, Geneva, 2024 <https://cds.cern.ch/record/2905239>.
- [32] CMS Collaboration, *Search for Higgs boson decays into Z and J/ψ and for Higgs and Z boson decays into J/ψ or Y pairs in pp collisions at $s=13 \text{ TeV}$* , *Phys. Lett. B* **842** (2023) 137534, [[arXiv:2206.03525](#)].
- [33] ATLAS Collaboration, *Search for the associated production of charm quarks and a Higgs boson decaying into a photon pair with the ATLAS detector*, [[arXiv:2407.15550](#)].

- [34] G. T. Bodwin, F. Petriello, S. Stoynev and M. Velasco, *Higgs boson decays to quarkonia and the $H\bar{c}c$ coupling*, *Phys. Rev. D* **88** (2013) 053003, [[arXiv:1306.5770](#)].
- [35] I. Brivio, F. Goertz and G. Isidori, *Probing the Charm Quark Yukawa Coupling in Higgs+Charm Production*, *Phys. Rev. Lett.* **115** (2015) 211801, [[arXiv:1507.02916](#)].
- [36] Y. Soreq, H. X. Zhu and J. Zupan, *Light quark Yukawa couplings from Higgs kinematics*, *JHEP* **12** (2016) 045, [[arXiv:1606.09621](#)].
- [37] J. A. Aguilar-Saavedra, J. M. Cano and J. M. No, *More light on Higgs flavor at the LHC: Higgs boson couplings to light quarks through $h + \gamma$ production*, *Phys. Rev. D* **103** (2021) 095023, [[arXiv:2008.12538](#)].
- [38] C. Delaunay, T. Golling, G. Perez and Y. Soreq, *Enhanced Higgs boson coupling to charm pairs*, *Phys. Rev. D* **89** (2014) 033014, [[arXiv:1310.7029](#)].
- [39] G. Perez, Y. Soreq, E. Stamou and K. Tobioka, *Constraining the charm Yukawa and Higgs-quark coupling universality*, *Phys. Rev. D* **92** (2015) 033016, [[arXiv:1503.00290](#)].
- [40] J. Walker and F. Krauss, *Constraining the Charm-Yukawa coupling at the Large Hadron Collider*, *Phys. Lett. B* **832** (2022) 137255, [[arXiv:2202.13937](#)].
- [41] Y. Nir and P. P. Udhayashankar, *Lessons from ATLAS and CMS measurements of Higgs boson decays to second generation fermions*, *JHEP* **06** (2024) 049, [[arXiv:2404.16545](#)].
- [42] N. Dong, H. Hou, Z. Qian, B. Wang and Q. Xu, *Probing Charm Yukawa through ch Associated Production at the Hadron Collider*, [arXiv:2407.19797](#).
- [43] D. Egana-Ugrinovic, S. Homiller and P. Meade, *Aligned and Spontaneous Flavor Violation*, *Phys. Rev. Lett.* **123** (2019) 031802, [[arXiv:1811.00017](#)].
- [44] G. C. Branco, W. Grimus and L. Lavoura, *Relating the scalar flavor changing neutral couplings to the CKM matrix*, *Phys. Lett. B* **380** (1996) 119–126, [[arXiv:hep-ph/9601383](#)].
- [45] A. Peñuelas and A. Pich, *Flavour alignment in multi-Higgs-doublet models*, *JHEP* **12** (2017) 084, [[arXiv:1710.02040](#)].
- [46] O. Eberhardt, A. P. n. Martínez and A. Pich, *Global fits in the Aligned Two-Higgs-Doublet model*, *JHEP* **05** (2021) 005, [[arXiv:2012.09200](#)].
- [47] A. Karan, V. Miralles and A. Pich, *Updated global fit of the aligned two-Higgs-doublet model with heavy scalars*, *Phys. Rev. D* **109** (2024) 035012, [[arXiv:2307.15419](#)].
- [48] Q. Bonnefoy, J. Kley, D. Liu, A. N. Rossia and C.-Y. Yao, *Aligned Yet Large Dipoles: a SMEFT Study*, [arXiv:2403.13065](#).
- [49] A. E. Nelson, *Naturally Weak CP Violation*, *Phys. Lett. B* **136** (1984) 387–391.
- [50] S. M. Barr, *Solving the Strong CP Problem Without the Peccei-Quinn Symmetry*, *Phys. Rev. Lett.* **53** (1984) 329.
- [51] L. Bento, G. C. Branco and P. A. Parada, *A Minimal model with natural suppression of strong CP violation*, *Phys. Lett. B* **267** (1991) 95–99.
- [52] G. Hiller and M. Schmaltz, *Solving the Strong CP Problem with Supersymmetry*, *Phys. Lett. B* **514** (2001) 263–268, [[arXiv:hep-ph/0105254](#)].
- [53] D. Egana-Ugrinovic, S. Homiller and P. R. Meade, *Higgs bosons with large couplings to light quarks*, *Phys. Rev. D* **100** (2019) 115041, [[arXiv:1908.11376](#)].

- [54] D. Egana-Ugrinovic, S. Homiller and P. Meade, *Multi-Higgs Production Probes Higgs Flavor*, *Phys. Rev. D* **103** (2021) 115005, [[arXiv:2101.04119](#)].
- [55] J. F. Gunion, H. E. Haber, G. L. Kane and S. Dawson, *The Higgs Hunter's Guide*, vol. 80. 2000.
- [56] S. Davidson and H. E. Haber, *Basis-independent methods for the two-Higgs-doublet model*, *Phys. Rev. D* **72** (2005) 035004, [[arXiv:hep-ph/0504050](#)].
- [57] N. Craig, J. Galloway and S. Thomas, *Searching for Signs of the Second Higgs Doublet*, [arXiv:1305.2424](#).
- [58] D. Egana-Ugrinovic and S. Thomas, *Effective Theory of Higgs Sector Vacuum States*, [arXiv:1512.00144](#).
- [59] J. F. Gunion and H. E. Haber, *The CP conserving two Higgs doublet model: The Approach to the decoupling limit*, *Phys. Rev. D* **67** (2003) 075019, [[arXiv:hep-ph/0207010](#)].
- [60] M. Misiak, A. Rehman and M. Steinhauser, *Towards $\bar{B} \rightarrow X_s \gamma$ at the NNLO in QCD without interpolation in m_c* , *JHEP* **06** (2020) 175, [[arXiv:2002.01548](#)].
- [61] HFLAV Collaboration, Y. S. Amhis et al., *Averages of b -hadron, c -hadron, and τ -lepton properties as of 2021*, *Phys. Rev. D* **107** (2023) 052008, [[arXiv:2206.07501](#)].
- [62] R. Bause, H. Gisbert, M. Golz and G. Hiller, *Model-independent analysis of $b \rightarrow d$ processes*, *Eur. Phys. J. C* **83** (2023) 419, [[arXiv:2209.04457](#)].
- [63] BABAR Collaboration, P. del Amo Sanchez et al., *Study of $B \rightarrow X \gamma$ Decays and Determination of $|V_{td}/V_{ts}|$* , *Phys. Rev. D* **82** (2010) 051101, [[arXiv:1005.4087](#)].
- [64] M. Ciuchini, M. Fedele, E. Franco, A. Paul, L. Silvestrini and M. Valli, *Constraints on lepton universality violation from rare B decays*, *Phys. Rev. D* **107** (2023) 055036, [[arXiv:2212.10516](#)].
- [65] T. Hermann, M. Misiak and M. Steinhauser, *$\bar{B} \rightarrow X_s \gamma$ in the Two Higgs Doublet Model up to Next-to-Next-to-Leading Order in QCD*, *JHEP* **11** (2012) 036, [[arXiv:1208.2788](#)].
- [66] A. Crivellin, A. Kokulu and C. Greub, *Flavor-phenomenology of two-Higgs-doublet models with generic Yukawa structure*, *Phys. Rev. D* **87** (2013) 094031, [[arXiv:1303.5877](#)].
- [67] A. Crivellin and L. Mercolli, *$B \rightarrow X_d \gamma$ and constraints on new physics*, *Phys. Rev. D* **84** (2011) 114005, [[arXiv:1106.5499](#)].
- [68] T. Hurth, E. Lunghi and W. Porod, *Untagged $\bar{B} \rightarrow X_{s+d} \gamma$ CP asymmetry as a probe for new physics*, *Nucl. Phys. B* **704** (2005) 56–74, [[arXiv:hep-ph/0312260](#)].
- [69] M. Czaja and M. Misiak, *Current Status of the Standard Model Prediction for the $B_s \rightarrow \mu^+ \mu^-$ Branching Ratio*, *Symmetry* **16** (2024) 917, [[arXiv:2407.03810](#)].
- [70] H. E. Logan and U. Nierste, *$B_{s,d} \rightarrow \ell^+ \ell^-$ in a two Higgs doublet model*, *Nucl. Phys. B* **586** (2000) 39–55, [[arXiv:hep-ph/0004139](#)].
- [71] M. S. Lang and U. Nierste, *$B_s \rightarrow \mu^+ \mu^-$ in a two-Higgs-doublet model with flavour-changing up-type Yukawa couplings*, *JHEP* **04** (2024) 047, [[arXiv:2212.11086](#)].
- [72] M. Ciuchini, M. Fedele, E. Franco, A. Paul, L. Silvestrini and M. Valli, *Charming penguins and lepton universality violation in $b \rightarrow s \ell^+ \ell^-$ decays*, *Eur. Phys. J. C* **83** (2023) 64, [[arXiv:2110.10126](#)].

- [73] M. Bordone, G. Isidori, S. Mächler and A. Tinari, *Short- vs. long-distance physics in $B \rightarrow K^{(*)}\ell^+\ell^-$: a data-driven analysis*, *Eur. Phys. J. C* **84** (2024) 547, [[arXiv:2401.18007](#)].
- [74] A. Crivellin, D. Müller and C. Wiegand, *$b \rightarrow s\ell^+\ell^-$ transitions in two-Higgs-doublet models*, *JHEP* **06** (2019) 119, [[arXiv:1903.10440](#)].
- [75] T. Inami and C. S. Lim, *Effects of Superheavy Quarks and Leptons in Low-Energy Weak Processes $k(L) \rightarrow \mu$ anti- μ , $K^+ \rightarrow \pi^+$ Neutrino anti-neutrino and $K^0 \leftrightarrow$ anti- K^0* , *Prog. Theor. Phys.* **65** (1981) 297.
- [76] UFIT Collaboration, M. Bona et al., *New UFit Analysis of the Unitarity Triangle in the Cabibbo-Kobayashi-Maskawa scheme*, *Rend. Lincei Sci. Fis. Nat.* **34** (2023) 37–57, [[arXiv:2212.03894](#)].
- [77] ATLAS Collaboration, *Search for heavy resonances decaying into a pair of Z bosons in the $\ell^+\ell^-\ell'^+\ell'^-$ and $\ell^+\ell^-\nu\bar{\nu}$ final states using 139 fb^{-1} of proton–proton collisions at $\sqrt{s} = 13\text{ TeV}$ with the ATLAS detector*, *Eur. Phys. J. C* **81** (2021) 332, [[arXiv:2009.14791](#)].
- [78] ATLAS Collaboration, *Search for resonant pair production of Higgs bosons in the $b\bar{b}b\bar{b}$ final state using pp collisions at $\sqrt{s} = 13\text{ TeV}$ with the ATLAS detector*, *Phys. Rev. D* **105** (2022) 092002, [[arXiv:2202.07288](#)].
- [79] ATLAS Collaboration, *Search for Higgs boson pair production in the two bottom quarks plus two photons final state in pp collisions at $\sqrt{s} = 13\text{ TeV}$ with the ATLAS detector*, *Phys. Rev. D* **106** (2022) 052001, [[arXiv:2112.11876](#)].
- [80] ATLAS Collaboration, *Search for resonant and non-resonant Higgs boson pair production in the $b\bar{b}\tau^+\tau^-$ decay channel using 13 TeV pp collision data from the ATLAS detector*, *JHEP* **07** (2023) 040, [[arXiv:2209.10910](#)].
- [81] CMS Collaboration, *Search for a new resonance decaying into two spin-0 bosons in a final state with two photons and two bottom quarks in proton-proton collisions at $\sqrt{s} = 13\text{ TeV}$* , [[arXiv:2310.01643](#)].
- [82] ATLAS Collaboration, *Search for heavy resonances decaying into a Z or W boson and a Higgs boson in final states with leptons and b-jets in 139 fb^{-1} of pp collisions at $\sqrt{s} = 13\text{ TeV}$ with the ATLAS detector*, *JHEP* **06** (2023) 016, [[arXiv:2207.00230](#)].
- [83] CMS Collaboration, *Search for Higgs boson pair production in the $bbWW$ decay mode in proton-proton collisions at $\sqrt{s} = 13\text{ TeV}$* , [[arXiv:2403.09430](#)].
- [84] J. Alwall, R. Frederix, S. Frixione, V. Hirschi, F. Maltoni, O. Mattelaer et al., *The automated computation of tree-level and next-to-leading order differential cross sections, and their matching to parton shower simulations*, *JHEP* **07** (2014) 079, [[arXiv:1405.0301](#)].
- [85] A. Alloul, N. D. Christensen, C. Degrande, C. Duhr and B. Fuks, *FeynRules 2.0 - A complete toolbox for tree-level phenomenology*, *Comput. Phys. Commun.* **185** (2014) 2250–2300, [[arXiv:1310.1921](#)].
- [86] S. Alte, M. König and M. Neubert, *Exclusive Weak Radiative Higgs Decays in the Standard Model and Beyond*, *JHEP* **12** (2016) 037, [[arXiv:1609.06310](#)].